MARMARA UNIVERSITY
FACULTY OF ENGINEERING

A ROOFTOP SOLAR PANEL DESIGN

MAHSUM AKGÖK

GRADUATION PROJECT REPORT

Department of Mechanical Engineering

Supervisor

Assoc. Prof. Dr. M. Rafet Özdemir

ISTANBUL, 2022

MARMARA UNIVERSITY

FACULTY OF ENGINEERING

A Rooftop Solar Panel Design

by

Mahsum Akgök

January 22, 2021, Istanbul

SUBMITTED TO THE DEPARTMENT OF MECHANICAL ENGINEERING

IN PARTIAL FULFILLMENT OF THE REQUIREMENTS FOR THE DEGREE

OF

BACHELOR OF SCIENCE

AT

MARMARA UNIVERSITY

Signature of Author Mahsum Akgök

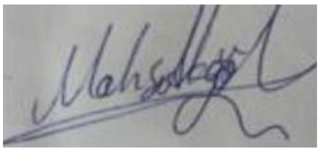

Department of Mechanical Engineering

Certified By.. Assoc. Prof. Dr. Mehmed Rafet ÖZDEMİR ....

Project Supervisor, Department of Mechanical Engineering

Accepted By...

Head of the Department of Mechanical Engineering

ACKNOWLEDGEMENT

First of all, I would like to express my deep and sincere gratitude to my research supervisor Assoc. Prof. Dr. Mehmet Rafet ÖZDEMİR for giving me the opportunity to do research and providing invaluable guidance throughout this research. His dynamism, vision, sincerity, and motivation have deeply inspired me. He has taught me the methodology to carry out the research. It was a great privilege and honor to work, and study under his guidance. I would also like to thank him for his friendship and empathy.

January 2022

Mahsum AKGÖK

CONTENTS

ACKNOWLEDGEMENT....i
CONTENTS....ii
ABSTRACT....iv
SYMBOLS....v
ABBREVIATIONS....vi
LIST OF FIGURES....vii
1. INTRODUCTION....1
2. SOLAR POWER....2
2.1. Solar Energy Potential in the World....2
2.2. The Energy Situation in Turkey and in the World....4
3. PV ENERGY SYSTEMS....5
3.1. Working Principle of PV Systems....6
4. MAIN TYPES OF SOLAR PANELS....11
4.1. Monocrystalline solar panels....11
4.2. Polycrystalline solar panels....11
4.3. Passivated Emitter and Rear Cell (PERC)....11
4.4. Thin-film solar panels....12
5. FACTORS AFFECTING PV EFFICIENCY....13
5.1. Tilt and Azimuth Angle....13
5.2. Optimal Azimuth Angle for Solar Panels....14
5.3. Finding the Optimal Tilt of the Solar Panels....16
6. PVSYST SIMULATION PROGRAM....17
6.1. Photovoltaic System Design....17
6.2. Input of Geographical Data into PVsyst Program....17
6.3. Description of Solar PV Grid System....19
6.4. Orientation of PV System....19
6.5. Selecting Inverter and PV Panels....20
6.6. Determining the PV Module to be Used in the System....21
6.7. Horizon Line Diagram....23
6.8. PVsyst Simulation Results....24
7. PVSYST MODULE PERFORMANCE MODEL....29

7.1. Data Methodology for PVsyst 30
7.2. Manuel Energy Calculation for Comparison 35
8. ECONOMIC ANALYSIS OF THE SYSTEM 36
8.1. Techno-Economic Feasibility Analysis 40
9. STRUCTURAL ANALYSIS OF THE ROOF FOR SOLAR PANEL DESIGN 41
9.1. Assessment of the Roof Structure 44
10. CONCLUSION 49
REFERENCES 50

ABSTRACT

Turkey is among the countries heavily dependent on energy imports. As a result of this dependency, the interest in new and alternative energy sources has increased. The installation of rooftop photovoltaic systems in Turkey is constantly increasing depending on geographical and meteorological conditions. This article presents a perspective on the potential situation for Turkey and a simulation study for rooftop photovoltaic systems design and calculation for my own home which is located in Bursa. This simulation study shows that a grid-connected rooftop photovoltaic system can generate a remarkable amount of power. The system is implemented in detail with PVsyst software. Detailed financial and performance analysis of the grid-connected rooftop photovoltaic system for the home with various parameters was also carried out in this study. Photovoltaic (PV) system installation in the building roof, which has an important potential in terms of solar energy and sunshine duration, is indispensable for clean energy requirements and is supported by simulation results. This document can be considered as a basic feasibility study before moving on to the implementation project.

SYMBOLS

I_L : photo-generated current (A)

I_O : dark saturation current (A)

γ : diode ideality factor (unitless)

V_{th} : thermal voltage for the module (V)

k : Boltzmann’s constant (1.38066×10^{-23} J/K),

q : elementary charge (1.60218×10^{-19} coulomb),

R_S : series resistance (Ω),

R_{SH} : shunt resistance (Ω)

E_0 : reference condition for irradiance ($1000 W / m^2$)

T_0 : reference condition for temperature ($298K$)

α : temperature coefficient for I_{SC} (A/K),

ε_G : effective band gap (eV),

μ_γ : temperature coefficient for the diode ideality factor (1/K),

$R_{SH,0}$: shunt resistance in the absence of irradiance (Ω),

$R_{SH,ref}$: shunt resistance at reference irradiance E_0 (Ω),

$R_{SH\exp}$: empirical term describing the change of shunt resistance with irradiance (unitless)

ABBREVIATIONS

BP **:** British Petroleum

IEA **:** International Energy Agency

LCC **:** Life Cycle Cost

LCOE **:** Levelized Cost of Energy

NREL **:** National Renewable Energy Laboratory

PERC **:** Passivated Emitter and Rear Cell

ROI **:** Return on Investment

LIST OF FIGURES

Figure 1. World Solar Energy Production (1989-2017) (Tw/H) (Bp, 2019 All Data) 3
Figure 2. World Solar Energy Potential For Pv Applications (Solargis, 2019) 3
Figure 3. Solar Energy Map Of Turkey [5] 5
Figure 4. Photovoltaic Power Potential Of Turkey [14] 5
Figure 5. Schematic Illustration Of A Pv Cell [22] 7
Figure 6. Typical Elements Of A Pv Energy System [23] 8
Figure 7. Tilt And Azimuth Angle In Relation To The Equator [17] 14
Figure 8. Pattern Of Magnetic Declination [17]... 15
Figure 9. Magnetic Declination Of Bursa Province [18] 16
Figure 10. Geographical Data Into Pvsyst 17
Figure 11. Coordinates Input Window 18
Figure 12. Window Of Geographic Coordinates Values 18
Figure 13. Grid Connected Pv System 19
Figure 14. Panel Angle And Azimuth Value Table For Pv Panels...................................... 20
Figure 15. Inverter Selection Screen 20
Figure 16. Efficiency Curve Of Inverter... 21
Figure 17. Pv Module Selection Screen 21
Figure 18. Panel Features 22
Figure 19. Panel Features 22
Figure 20. PV Module Characteristic Curve 23
Figure 21. Azimuth And Corresponding Height Values[24] 24
Figure 22. Horizon Line Diagram 24
Figure 23. Monthly Change Graph Of Performance Ratio 25
Figure 24. Pv Cell Temperature/Efficiency Graph... 25
Figure 25. General Results 26
Figure 26. Loss Diagram For The Whole Year.. 27
Figure 27. Shading Scene Construction 28
Figure 28. Shading Loss... 28
Figure 29. Investment Costs 37
Figure 30. Investment Costs 38
Figure 31. Operating Costs... 39
Figure 32. Financial Parameters 39

Figure 33. A Flowchart Summarizing Our Techno-Economic Evaluation Methodology 40
Figure 34. Roof Collapse Due To Excessive Snow Load [26] 41
Figure 35. Truss Failure Due To Excessive Roof Load [26] 42
Figure 36. Bending In The Beam [26] 43
Figure 37. Axial Load In The Column [26] 43
Figure 38. Vertical Load Path For Gravity Loads [27] 45
Figure 39. Vertical Load Path For Wind Uplift [27] 46
Figure 40. Weight Loading Calculation On Easypv Tool 47
Figure 41. Structural Calculations Of The Design 48

LIST OF TABLES

Table 1. Generation And Goals Of Energy (Res: Renewable Energy Sources) (Mw) [4].......4
Table 2. Charge Controller Types And Comparison [21] 9
Table 3. Inverter Types And Comparison [15] 9
Table 4. Battery Types And Comparison [8] 11
Table 5. Types Of Solar Panels And Comparison [16] 12
Table 6. Dead Loads For Common Residential Construction [27] 47

1. INTRODUCTION

Nowadays, we live in a world where every aspect of life grows almost at the speed of light. The size of all populations increases incredibly along with their use of all sorts of energy to fulfill their fundamental needs. Thus, there is an urgent need for new and further sources of energy to complete this task. Furthermore, there is also a perceptible development in the field of technology which is controlling the flow of some parts of our lives. In fact, this is the era of development and technology and we can't live without this technology. For example, we can see people from the youth to the aged ones using the internet and smartphones everywhere we go. All this progress pushes researchers and scientists to make our lives more comfortable by providing new and better tools that we can use as basics.

In the past years, people used to ride horses instead of driving cars; send letters instead of texting or sending emails and use natural resources like wood and rocks to stay warm instead of using air-conditioners. From here, we can see the great change and the advantages and impact of technology on our lives that makes everything faster and more affordable. Therefore, all types of sources of energy are crucial for our well-being.

Today, energy is one of the most current problems of the whole world. Increasing human needs every day increases the demand for energy. On the other hand, due to the increase in the amount of production as the world population increases, energy production should also increase regularly. The rapid economic growth experienced in some countries rapidly increases the energy needs of the countries. In such countries, the need for energy in industry, residences, and transportation increases relatively every year. The role of energy in the life of societies is important: it plays an active role, from direct or indirect economic development to the development of social welfare.

There are many different types of energy in nature. The main ones are chemical, nuclear, mechanical (potential and kinetic) and thermal energies. On the other hand, there are many energy sources in nature: the main ones are fossil-derived sources, hydraulic, solar, wind, geothermal, wave and biofuels. In addition to these, hydrogen, on which intensive studies have been carried out, especially in recent years, emerges as an important energy vector. Energy resources are divided into two groups in terms of the continuity of resources in nature; These are non-renewable resources that are present in nature in a certain amount and cannot be replaced when used, and renewable resources that exist on a continuum in nature. Energy can be categorized as primary and secondary sources in terms of the availability of energy in nature or its conversion from other energies. The first of these are found in nature, such as oil, natural gas, coal, biomass, the sun, and wind. Secondary energy is obtained as a result of the conversion of primary energy sources. Examples of secondary energy sources are electricity, gasoline, diesel, and LPG.

Renewable energies are regarded as the future of our generation; it is an expanding field that has many positive and important impacts on our lives. As a future engineer, I want to leave a footprint and participate in the improvement of science by contributing to the results of my current project. Besides this, I am really interested in the mechanical engineering department and specifically the recent field of renewable energy applied to solar power technology that is becoming a tendency lately.

2. SOLAR POWER

The Sun is a densely hot gaseous sphere with a diameter of 1.39×10^9 m and is approximately 1.5×10^{11} m away from Earth. While the temperature on the surface of the sun is 5500 ˚C, it reaches 15.6 million ˚C in its centre. While the diameter of the sun is 109 times the diameter of the earth, its volume corresponds to 1.3 million times that of the earth. Only 50% of the sun's rays (sun beams) reach the earth. About 30% is reflected back by the atmosphere.[19]

Only one in 2.2 billion of the energy emitted from the sun reaches the earth, and this energy constitutes the basic energy source necessary for life. The intensity of solar energy outside the Earth's atmosphere is 1370 W/m^2 on average, but the amount reaching the earth varies between 0-1100 W/m^2 due to the atmosphere. In one second, 4 million tons of mass from the sun is converted into energy. Since the sun will continue to shine for millions of years, it will continue to be an endless source of energy for our world.[20]

Solar energy is among the cleanest energy sources. Solar energy is environmentally advantageous compared to other energy sources. It is renewable, does not cause CO_2 or other gaseous emissions, and does not produce liquid or solid waste.

2.1. Solar Energy Potential in the World

The energy source that has the largest share among renewable energy sources is hydraulic energy, as well as solar and wind energy investments and installed power have increased significantly in recent years. According to the International Energy Agency (IEA) data, solar energy will receive an investment of 116 billion dollars until 2030 within the current policies, 125 billion dollars in the 2031-2040 period, approximately 180 billion dollars until 2030, and 191 billion dollars in the 2031-2040 period according to the sustainable policies scenario. [21]

This situation is clearly seen when the amount of solar energy production and installed power in global electricity production is examined. Both the amount of electricity generation from solar energy and the rates of installed power continue to increase compared to the previous year.

According to British Petroleum (BP) data, solar power generation, which was below 1 MW at the end of the 1980s, reached 584 million MW as of 2018. In terms of installed power values, according to BP data, solar energy installed power, which was only 424 MW at the end of the 1990s, reached 488 thousand MW in 2018. [19]

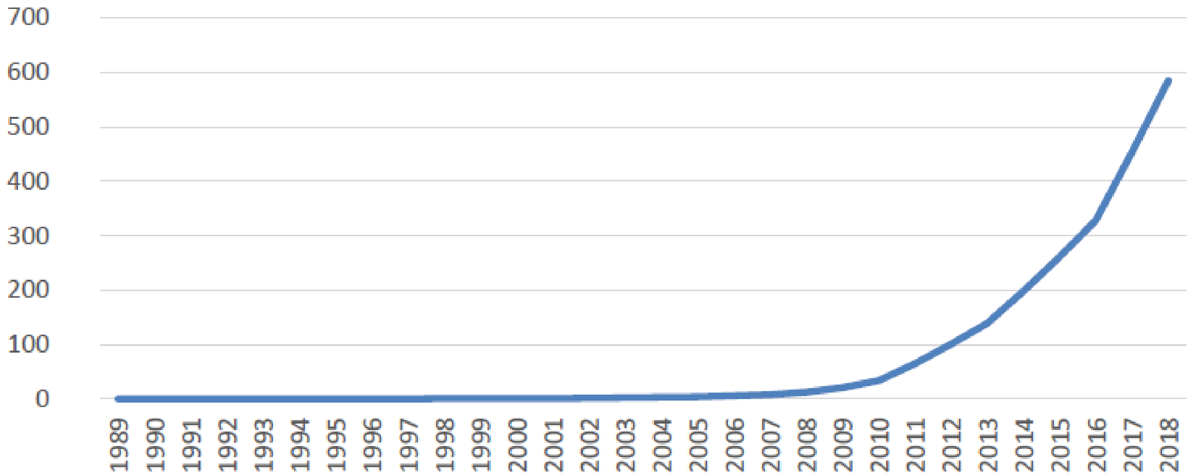

Figure 1. *World Solar Energy Production (1989-2017) (TW/h) (BP, 2019 all data)*

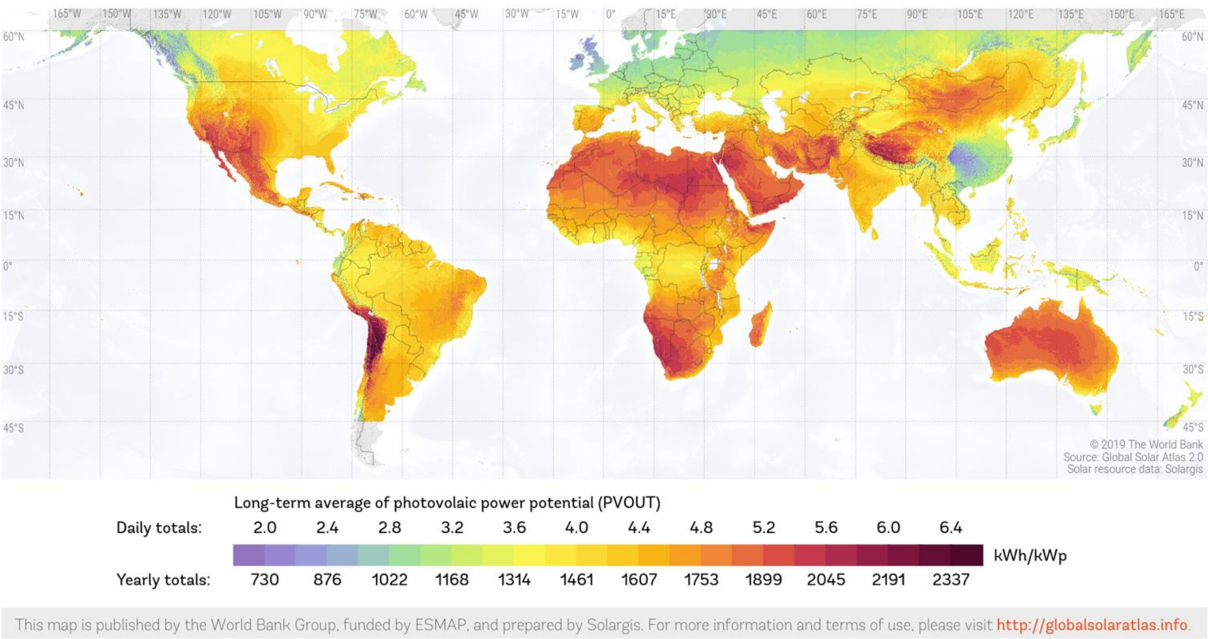

Figure 2. *World Solar Energy Potential for PV Applications (SOLARGIS, 2019)*

Every country has the potential to benefit from solar energy. However, from the point of view of PV applications, the most useful geography of the world, the regions between 35˚ north and 35˚ south latitudes of the equator and known as the “Earth-Sun Belt” are shown in Figure 2.

2.2. The Energy Situation in Turkey and in the World

When the grid-connected PV systems are considered in the world, China is the leader with 131,000 MW installed power capacity. United States is in the second order with the 51,000 MW and Japan is the third with an installed power capacity of 49,000 MW. And Turkey ranks 12th with 5,095 MW installed power capacity. The generation of electricity with existing and planned PV power plants in Turkey continues to increase. PV energy generation was 4.5 GWh in the time period between January-May 2014, and it was 32.3 GWh in the same period of 2015, was 266.6 GWh in the same period of 2016, and was 844.56 GWh in the same period of 2017 [1]. When we examine the number of PV power plants, the growth rate commissioned in 2014 was 223% if we compared it to the previous year [2]. 20,000 MW of wind energy, 5,000 MW of solar energy, 1,000 MW of biomass energy, 34,000 MW of hydropower, and 1,000 MW of geothermal energy are planned to be generated in Turkey within the scope of the 2023 goals. Energy generation and goals related to renewable energy sources are given in Table 1. According to these goals, it is planned to provide at least 30% of Turkey’s demand for electrical energy (including hydropower) from renewable energy sources until 2023. Approximately $60 billion is expected to be invested in renewable energy sources to achieve this goal [3].

Table 1. *Generation and Goals of Energy (RES: Renewable Energy Sources) (MW) [4]*

RES	2015	2017	2019	2023
Hydro	25526	28763	32000	34000
Wind	5660	9549	13308	20000
Solar	300	1800	3000	5000
Geothermal	412	559	706	1000
Biomass	377	530	683	1000

Turkey is located in the world between 36^0-42^0 north latitude and 26^0-45^0 east longitude. Turkey's annual average solar radiation is 1303 kWh/m^{2}year (Figure 3), and the average annual sunshine duration is 2623 hours. This figure corresponds to a power of 3.6 kWh/m^2 per day, approximately 7.2 hours of sunshine per day, and 110 days of sunshine for collection.

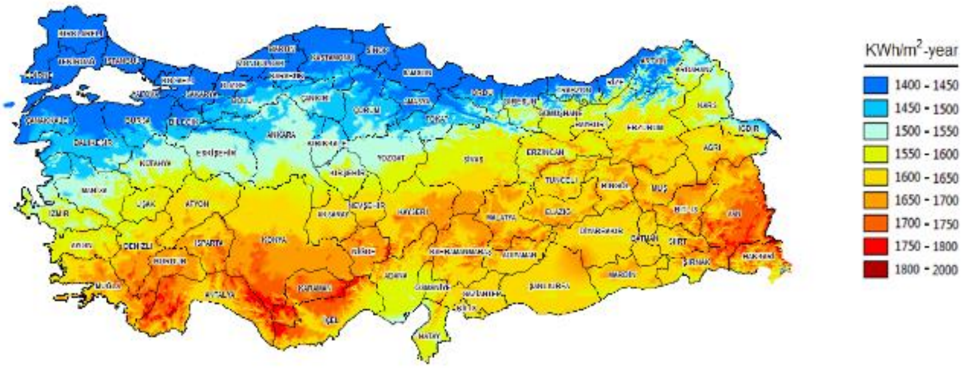

Figure 3. *Solar Energy Map of Turkey [5]*

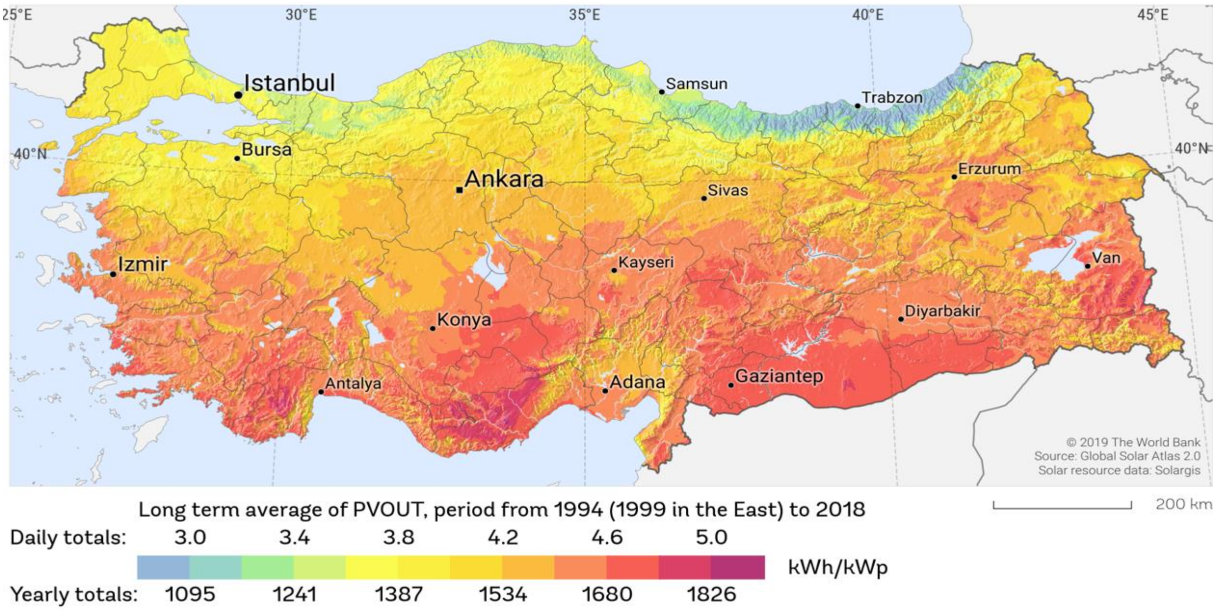

Figure 4. *Photovoltaic Power Potential of Turkey [14]*

3. PV ENERGY SYSTEMS

The PV effect was first discovered in 1839 by the French Physicist Edmond Becquerel during his studies on platinum layers. Mankind's interest in using solar energy goes back more than 100 years. In the early days, solar energy was used only to produce the steam necessary for the operation of some machines. Edmond Becquerel later discovered the PV effect, which would convert sunlight into electrical energy.

In 1873, scientist Willoughby Smith discovered photoconductivity in selenium, and this invention made history as the first PV assembly. As a result of these developments, solar energy has been converted into electricity and used more effectively. In 1883, Charles Fritts developed a PV cell with 1% efficiency. The physical mechanism of the PV effect was discussed by Albert Einstein in 1905 and Einstein was awarded the Nobel Prize in Physics in 1921. [6]

Russell Ohl patented the modern PV solar panel in 1946. American researcher Russell Ohl, working at Bell Laboratories, obtained 6% efficient silicon PV cells in 1954. Hoffman Electronics company developed silicon PV cells in 1958 that can operate with 9% efficiency. In the same period, one of the first applications of electricity generation from PV cells was carried out on the Vanguard-I spacecraft. In the following years, the first PV plant with an installed capacity of 1 megawatt was built in Hesperia California in 1982 [6]. Seven years later, in 1989, efficiencies were now over 19% and a new high-efficiency method, double-jointed PV cells, was introduced by Applied Solar Energy Corp. company and in 1993 the same company started mass production of 20% efficient cells. Three-junction PV cells with 20% efficiency in 2000 and then 28% efficiency in 2005 were developed. In the following period, Spectrolab company succeeded in developing three-junction PV cells with 40% efficiency in 2006 and NREL 40.8% efficiency in 2008. One year after this development, Spectrolab company broke the world record by developing 41.6% efficient triple-joint PV cells in 2009.

3.1. Working Principles of PV Systems

PV cells are a converter made up of different types of semiconductor structures. The basic structure of PV cells is based on the juxtaposition of (-) N-type, whose charge carriers are mostly electrons, and (+) P-type semiconductors, whose charge carriers are mostly holes.

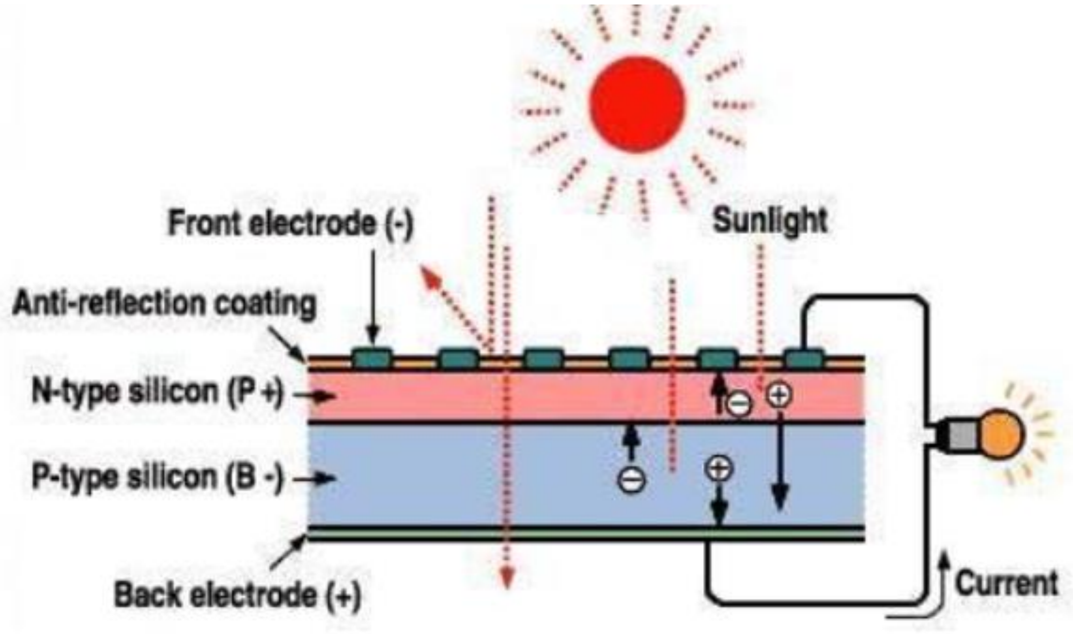

Figure 5. *Schematic Illustration of a PV Cell [22]*

A schematic representation of a PV cell is given in Figure 5. As seen in the figure, if the photons with sufficient energy fall on the junction point, the electrons can jump to the conduction band and create a current. In this way, in the P-N semiconductor region, the holes pass from the P-type region to the N-type region and the electrons from the N-type region to the P-type region through the P-N junction (diffusion current). Ions fixed near the P-N junction site create an electric field opposite to diffusion, causing a drift current. After that, the diffusion current and the drift current are balanced, making the net current equal to zero. With this, a potential barrier is established at the P-N junction. Therefore, when sunlight falls on the PV cells, the electrons absorb the energy of the photons. With this, the bonds of the electrons are broken and the separated electrons produce hole pairs. These charge carriers are repelled by the electric field through the P-N junction. The electron-hole pairs separated from each other by the electric field create a power output between the contact ends of the PV panel. If an external load is connected, electric current and potential differences arise between the cell terminals.

PV cell and module efficiencies have different meanings. The efficiency of the PV cell is higher than the efficiency of the PV module. For example, while the efficiency of a single crystal silicon cell is 24%, the efficiency of a module consisting of the same cells can be between 13−17%. While the efficiency of the polycrystalline silicon cell is 18%, the module efficiency is between 11−15%. The reason for this is that the module efficiency calculation is made by considering the entire panel surface. Depending on the type of crystal the module is made of the yields of commercial ones vary between 15% and 20% on average and between 10-30% under laboratory conditions. Only under standard operating conditions, solar modules operate at nominal power. Some reasons affect the energy-generating efficiency of modules. Some of these can be expressed as pollution of the panel surfaces, the angle of incidence of the sun's rays not being perpendicular; partial shading, and module temperature. [21]

There are typical elements of PV systems used in residences for the required electricity generation. However, these elements may differ in terms of the characteristics and needs of the system. Typical elements are generally PV panels, charge controller, inverter, and batteries.

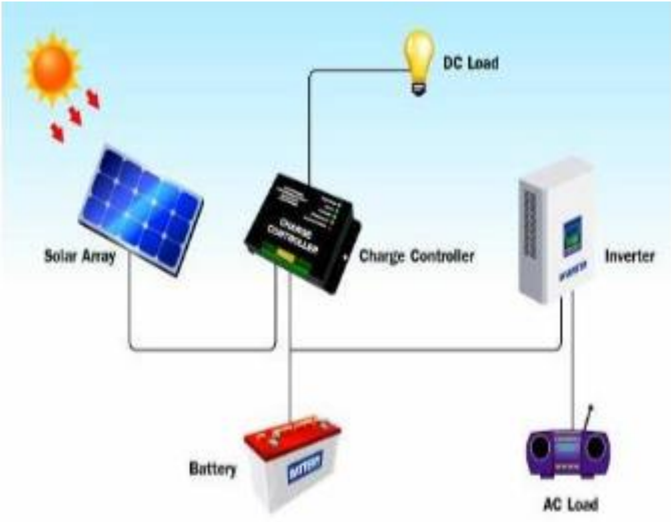

Figure 6. *Typical Elements of a PV Energy System [23]*

Charge Controller

The main task of the charge controller is to charge the batteries and prevent high discharge. It stabilizes the DC energy from the solar module and creates stable DC electrical energy necessary for charging the batteries. There are two types of charge controllers in the market today, Pulse Width Modulation (PWM) and Maximum Power Point Tracking (MPPT) compared in Table 2. While PWM charging is more complex, they are more durable as they do not have any breakable mechanical connections. MPPT charge controls, on the other hand, lose less power, are more expensive, and have significantly improved performance. Therefore, it is highly recommended. Besides, failure of charge controllers may require battery replacement and maintenance costs are quite high.

Table 2. *Charge Controller Types and Comparison [21]*

	Cost	**Efficiency**	**Endurance(Life Cycle)**	**Environment and Recommended Use**
PWM	Low	Lower	Longer lifespan due to less components that may break	Best in warm sunny days
MPPT	High	Higher	Shorter lifespan due to more components	Best in colder, cloudier environments

Inverters

Inverters are electronic devices that convert DC (direct current) electrical energy into AC (alternating current) electrical energy. In the input part of the inverters, direct current sources such as batteries, PV cells, fuel cells, or the outputs of rectifiers fed from an alternative source can be used. In general, inverters can be single-phase or three-phase. In addition to this, there are three types of inverters a square wave, sine, and full sine in inverters fed from renewable energy sources and on-grid PV systems. Square wave and sine wave inverters are compared in Table 3.

Table 3. *Inverter Types and Comparison [15]*

List of Features	**Square Wave Inverter**	**Sine Wave Inverter**
Supported Appliances	Square wave inverters are usually used to support motors alone.	Sine wave inverters are used to support household appliances such as refrigerators ovens, computers, laptops, etc.
Overall Safety Level	Square wave inverters are less reliable and also unsafe to use for appliances.	Sine inverters are highly safe to use.
Noise Interference	Square wave inverters produce a very loud noise when used.	Sine wave inverters produce normal sound only.
Cost	Square wave inverters are less expensive than Sine wave inverters.	Sine wave inverters are more expensive than Square wave inverters.

Batteries

One of the most important elements of PV systems are batteries. Battery cost for a typical system is 15-20% of the total system cost. On the other hand, the average life of PV modules is 15-20 years, while the average lifespan of lead acid batteries is 2-3 years. Although the maintenance cost of PV systems is almost non-existent, the short life of the batteries is the most important factor that increases the system cost. In addition, studies are continuing on Nickel-Cadmium, Nickel-Hydrogen, Nickel-Metal Hydrate, Zinc, Zinc-Bromide, Zinc-Manganese dioxide, Zinc-air, Sodium-Sulphur, Lithium, and redox batteries.

Lithium-ion batteries are one of the most preferred batteries on the market today.

Lithium-Ion Batteries

Lithium was discovered in 1817 by Arfwedson and Berzelius while analysing petalite ore, but its acceptance as an element was achieved in 1821 by Brande and Davy, when it was isolated by electrolysis of a lithium oxide. But Lewis began discovering its electrochemical properties a century later. Lithium-polycarbonic monofluoride batteries were introduced commercially by Matsushita in 1973 and lithium-manganese oxide batteries by the Sanyo company in 1975. In the early days, these batteries were applied in calculators that could be charged with solar energy and offered for sale. Later, with the development of battery technology, a rechargeable battery (secondary) type, which differs in usage areas, capacities, and features, has emerged.[7]

Comparison of Lithium Ion and Lead Acid Batteries

Today, the usage areas of lithium-ion batteries are mostly power systems applications, the automotive sector, and PV systems. Li-ion batteries, especially LiFeSO4 batteries, are technically more advantageous compared to traditional lead-acid batteries in PV systems in terms of fast charging rate, high energy density, long cycle life, high safety, and also low maintenance as compared in table 4. On the other hand, the high cost of Li-ion batteries can be said to be at a disadvantage. Li-ion batteries require approximately 2-3 hours to fully charge, while lead-acid batteries take approximately 12-16 hours. On cloudy and low irradiation days, lead-acid batteries need more time to fully charge than Li-ion batteries as the output of the PV module is reduced. Therefore, the low PV output may be insufficient to fully charge such batteries. If this scenario continues like this, the performance of the lead-acid battery will decrease. However, a low state of charge (SoC) is not a problem for Li-ion batteries. Therefore, the use of Li-ion batteries in PV systems provides more advantages. Another advantage of Li-ion batteries is that they have a longer cycle life. The cycle life of the lead acid battery varies between 500-1000, while the cycle life of the Li-ion (LiFeSO4) battery is between 2000-5000. Cycle life, depth of discharge (DOD), discharge rate and temperature are the most important factors of batteries, while lead acid batteries are more sensitive to these factors. Since the cycle life is affected by DOD, a lead acid battery of the same size with 30% DOD can have the same cycle life as a Li-ion battery with 75% DOD. This shows that the lead acid battery needs to be 2.5 times larger to achieve comparable cycle life.[8]

Table 4. *Battery Types and Comparison [8]*

	Cost	Efficiency	Endurance(Life Cycle)	Charge Time
Battery li-ion	High	High (≥%95)	High (2000-5000)	Low(2-3 hours)
Battery lead acid	Low	Lower(%80-85)	Low (500-1000)	High (12-16 hours)

4. MAIN TYPES OF SOLAR PANELS

Nowadays, there are 4 major types of solar panels available on the solar panel market, monocrystalline, polycrystalline, PERC, thin-film panels.

4.1. Monocrystalline Solar Panels

They are also known as single-crystal panels; these are made from a single pure silicon crystal which is cut into several wafers. Since they are made from pure silicon, they can be readily identified by their dark black color.

4.2. Polycrystalline Solar Panels

These types of panels consist of different silicon crystals instead of one. The silicon fragments are melted and poured into a square mold. This makes polycrystalline cells much more affordable since there is hardly any wastage and gives them that characteristic square shape.

4.3. Passivated Emitter and Rear Cell (PERC)

PERC stands for “passivated emitter and rear contact” or “rear cell”. Solar panels built with PERC cells have an additional layer on the back of the traditional solar cells. This additional layer allows more sunlight to be captured and turned into electricity, making PERC cells more efficient than traditional cells.

4.4.Thin-Film Solar Panels

Thin-film panels are characterized by very fine layers that are thin enough to be flexible. Each panel does not require a frame backing, making them lighter and easier to install.

Table 5. *Types of Solar Panels and Comparison [16]*

	PERC	**Monocrystalline**	**Polycrystalline**	**Thin film**
Initial Cost	Highest	High	Middle	Highest to lowest: CIGS CdTe a-Si
Efficiency	Highest (5% more than monocrystalline)	20% and up	15-17%	CIGS: 13-15% CdTe: 9-11% a-Si: 6-8%
Appearance	Black with rounded edges	Black with rounded edges	Blue with square edges	Depends on the thin-film variant
Advantages	Requires least space Most efficient Highest power capacity	Less expensive alternative to PERC panels without the passivating layer	Middle option in terms of cost, efficiency, and power capacity	Lowest cost Easier to install
Disadvantages	Most expensive Some earlier panels suffered from light and elevated temperature induced degradation	High initial cost Low yield in the manufacturing process	Low heat tolerance, not suitable in hot environments	Shorter lifespan than crystalline panels requires more space Least efficient

5. FACTORS AFFECTING PV EFFICIENCY

The power produced by PV panels varies due to environmental conditions such as solar radiation intensity and temperature. Tilt and azimuth angles are also important in process of PV systems. At the same time, it is very important that PV systems are operated in such a way as to obtain maximum power since the efficiency rate of PV systems is not high and the installation costs are more expensive than traditional electricity generation systems. Therefore, it is important to determine the maximum power to be produced by PV systems, whose efficiency varies due to environmental conditions such as solar radiation intensity or temperature, and to operate them at maximum power at the same time.

The solar energy potential of a region depends on the sunshine duration and solar radiation value of the region. Turkey's annual average sunshine duration is 2482 hours [12] and the annual average solar radiation value is 1583.5 kWh/m2 [13]. This value increases considerably as you go south. Apart from this, outdoor air temperature and wind speed are local climate characteristics that affect panel performance. PV panels convert a very small part (maximum 20%) of the solar energy coming on them into electrical energy. The rest is released as heat. As a result, the panel surface's temperature is constantly increasing during the generation of electrical energy in PV panels. This is an important factor that negatively affects panel performance.

5.1. Tilt and Azimuth Angle

The "tilt angle" or "elevation angle" describes the vertical angle of the solar panels and "Azimuth angle" is their horizontal facing in relation to the Equator.

Designed solar panels should face directly into the sun to optimize their output. In this part, it will be seen how to find the right tilt and azimuth angle to get the most production out of your array.

- Elevation Angle: The vertical tilt of the panels.
- Azimuth Angle: The horizontal orientation of the panels (in relation to the equator, in this case).

Solar panels work best when these panels face directly into the sun. But creating such a design is a little complicated by the fact that the sun moves across the sky throughout the day. It also changes the angle in the sky as the seasons change.

So when designing a solar PV system, one of the most important questions is: what's the best angle to mount the solar panels to get the highest efficiency from the design?

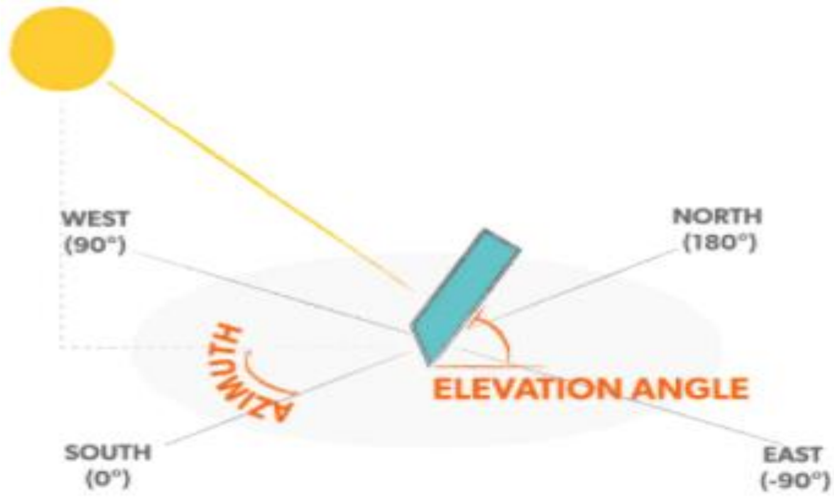

Figure 7. *Tilt and azimuth angle in relation to the Equator [17]*

5.2. Optimal Azimuth Angle for Solar Panels

On the roofs, it is seen some solar panels are set at one angle and never change, while some designers make adjustments to optimize output.

The tracker may be purchased for a more efficient panel design, which automatically follows the sun's position within the sky to get the most output from the panels. But trackers are rarely the most cost-effective option. It's nearly always cheaper to buy a few more panels rather than investing in a tracker.

For best results, the solar panels should face toward the equator. If we live in the Northern hemisphere, we face them south. If we live in the Southern hemisphere, we face them north for better efficiency (output). Since we live in Turkey, which is located in the Northern hemisphere, we will point our system to the south to get better output.

Many people are surprised to be told that their compass isn't completely accurate. That happens because magnetic forces within the Earth's core pull the compass needle away from true north or true south. Depending on the location, the compass reading can be inaccurate by the maximum amount as 25°. [17]

The difference between magnetic north (the reading on the compass) and true north is known as magnetic declination. This is a measurement of how many degrees need to compensate from the compass reading to find true north.

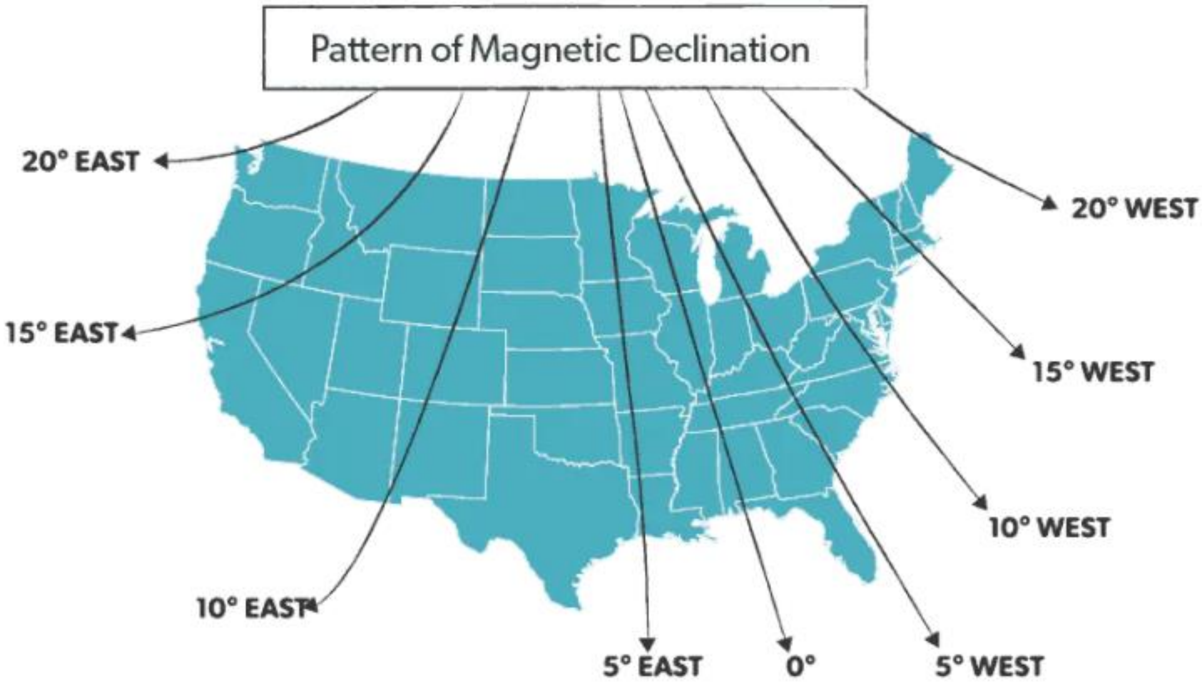

Figure 8. *Pattern of Magnetic Declination [17]*

For the ideal azimuth angle for the panels; firstly, magnetic declination can be found from tool like given at [18].

Adjust the facing of the panels by the magnetic declination value in the location of the project. The direction you adjust the panels depends on where you live:

In the Northern Hemisphere:

- If the magnetic declination is east (positive), rotate the panels east.
- If the magnetic declination is west (negative), rotate the panels west.

In the Southern Hemisphere:

- If the magnetic declination is east (positive), rotate the panels west.
- If the magnetic declination is west (negative), rotate the panels east. [18]

In the figure given below, we can see that the magnetic declination of Bursa is about 6° east. Since Bursa is in the Northern hemisphere, we start by finding the magnetic south, then adjust 6° to the east to find the ideal azimuth.

By performing such an adjustment, the panels will be facing directly at the equator, maximizing their exposure to sunlight (and by extension, the amount of solar power generated).

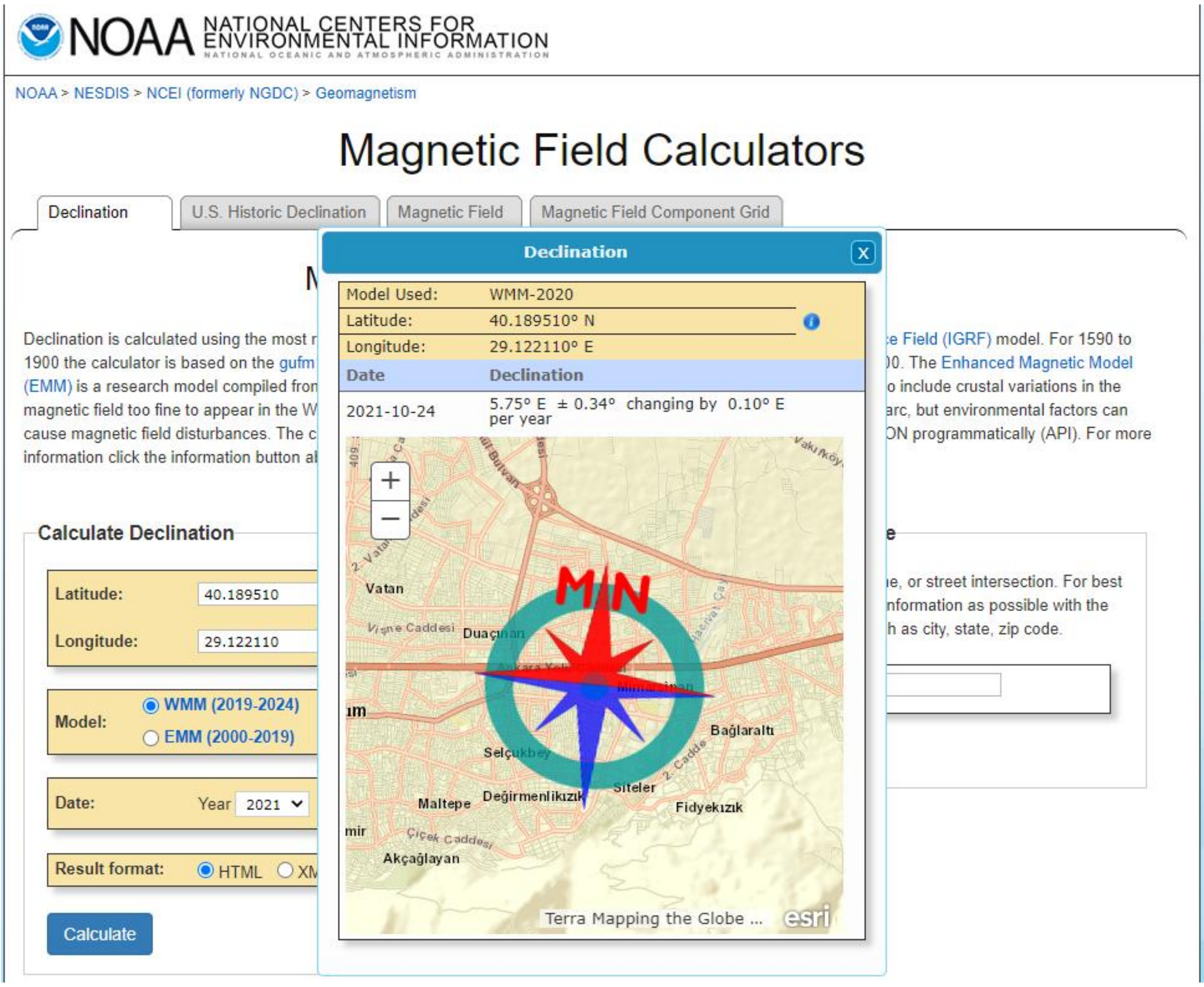

__Figure 9.__ Magnetic Declination of Bursa Province [18]

5.3. Finding the Optimal Tilt of the Solar Panels

One of the useful approach for tilt angle of panels is that setting their angles equal to latitude of the design location.(in the Bursa province it can be taken 40°)

To optimize overall production year-round, tilt the panels at design area's latitude. (Also suitable for spring and autumn periods)

To lean toward more production in the summer, tilt the panels at latitude minus 10-15°.

To lean toward more production in the winter, tilt the panels at latitude plus 10-15°. [17]

6. PVSYST SIMULATION PROGRAM

The PVsyst program is a simulation program developed by the University of Geneva, Switzerland, for the purpose of making photovoltaic system designs such as grid-connected or off-grid PV systems, PV irrigation systems and DC networks, and examining the results. This program is more practical than the other solar panel design software programs because it allows more detailed calculations and the use of different parameters.

6.1. Photovoltaic System Design

The realization of a grid connected and energy storage PV (Photovoltaics Photovoltaic) system with the PVsyst program is briefly explained below.

6.2. Input of Geographical Data into PVsyst Program

Geographical location data is entered in the following order.

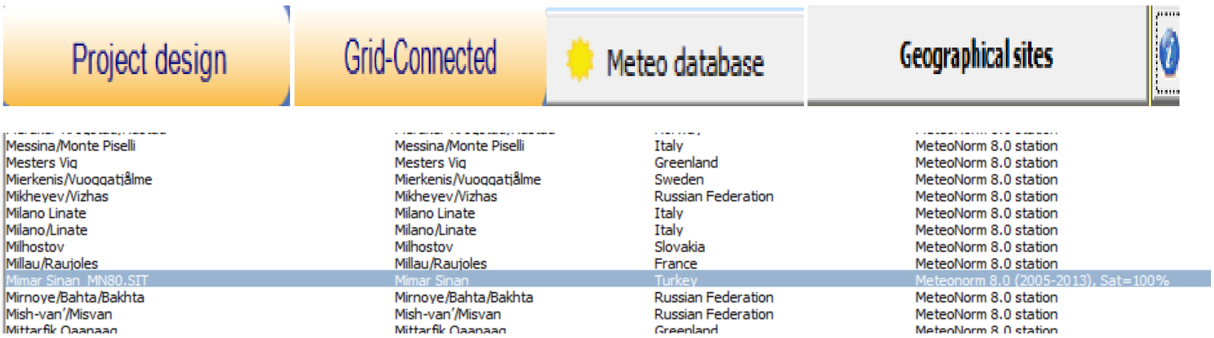

Figure 10. *Geographical Data into PVsyst*

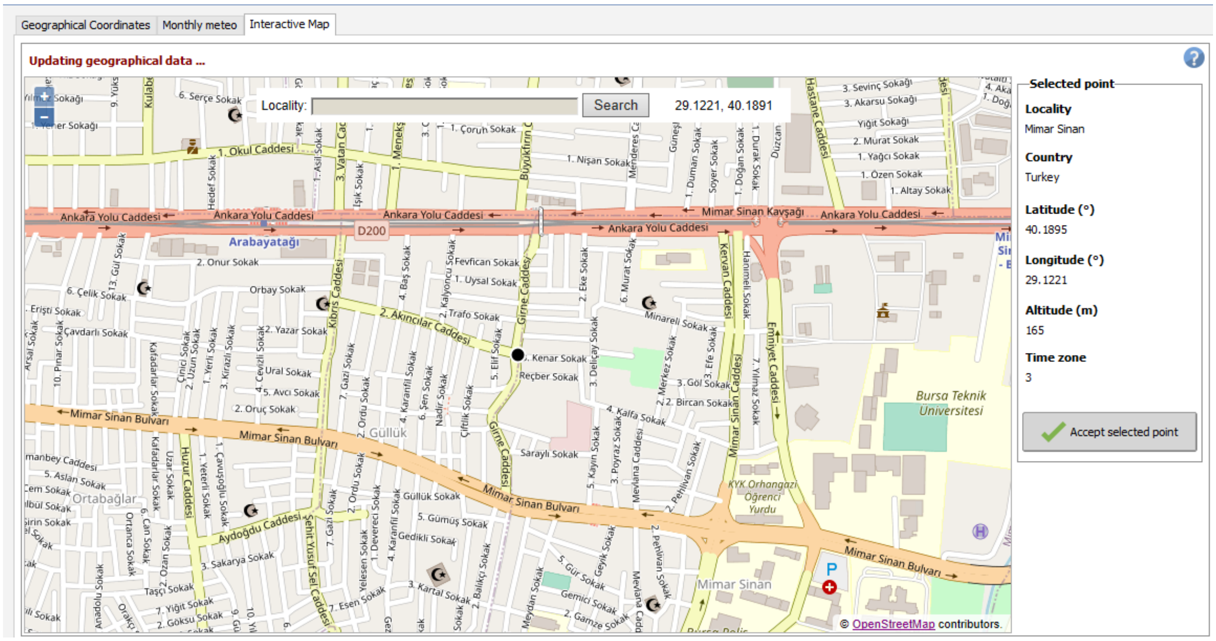

Figure 11. Coordinates Input Window

After the desired location is determined as in Figure 11, the geographic location information is entered by pressing ‘‘Accept selected point’’.

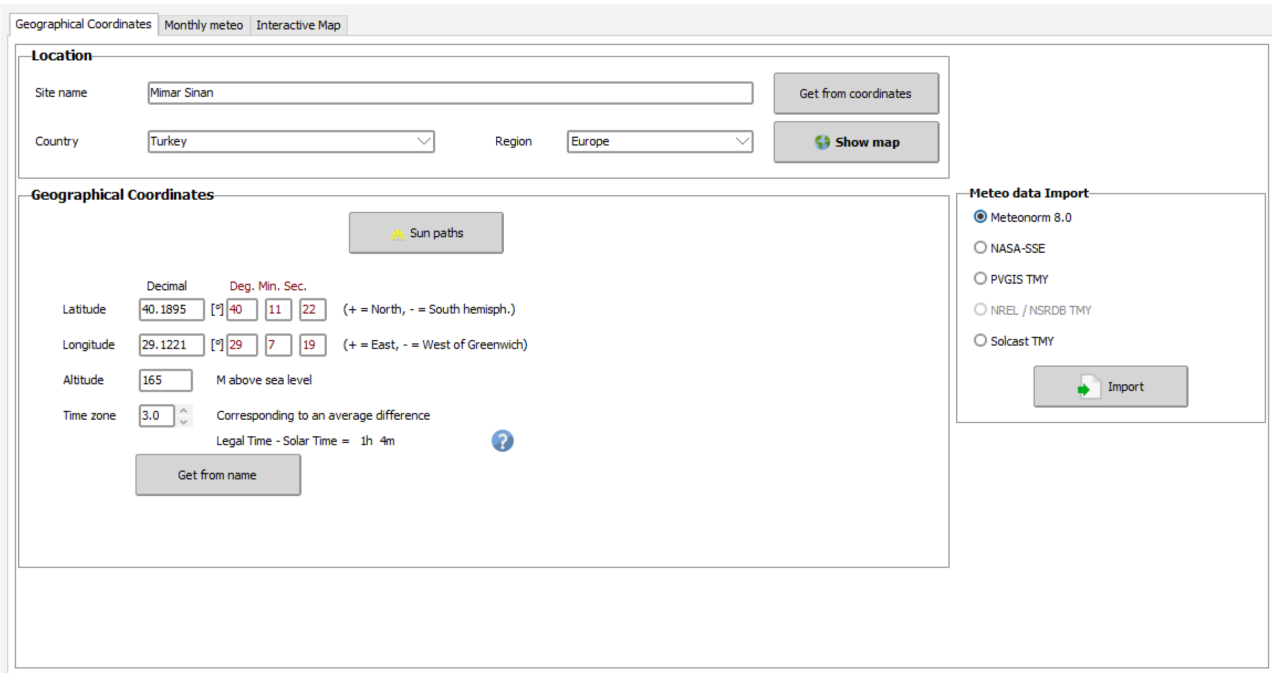

Figure 12. Window of Geographic Coordinates Values

6.3. Description of Solar PV Grid System

A grid-connected PV system; It consists of solar panels, inverters, a power conditioning unit and grid connection equipment. Since there will be no losses for energy storage, it ensures that the power produced from solar energy is used effectively. The proposed model is shown in Figure 10 with the PV system software.

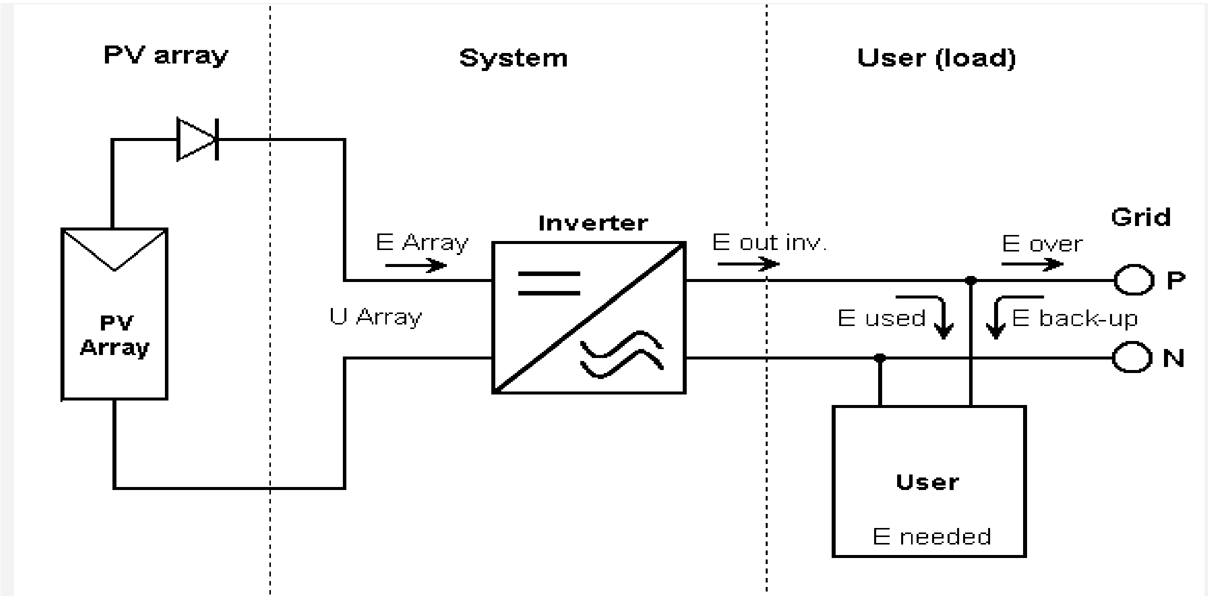

Figure 13. *Grid Connected PV System*

6.4. Orientation of PV System

By pressing the 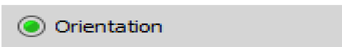

button, the PV system can be adjusted.

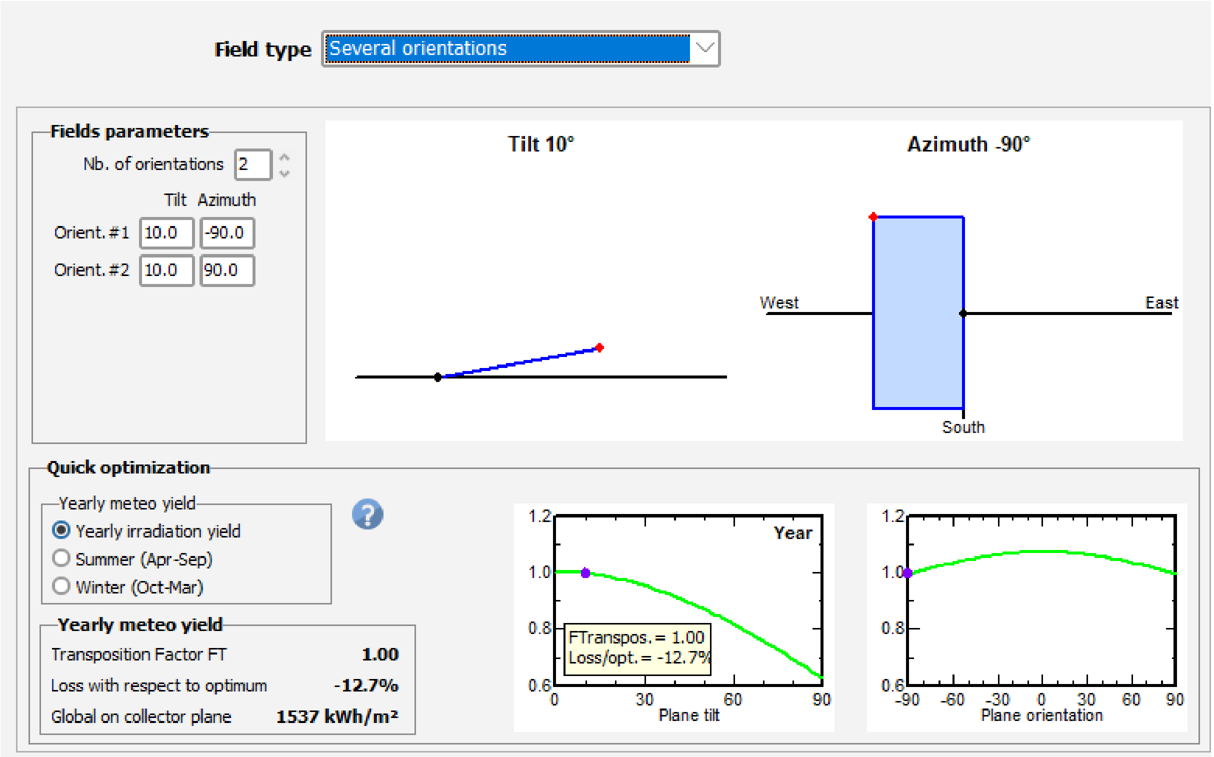

Figure 14. *Panel Angle and Azimuth Value Table for PV Panels*

As it seen figure 14 we choose azimuth angle as 90° and -90° because our design will be east-west oriented.

6.5. Selecting Inverter and PV Panels

At the stage of obtaining energy using photovoltaic panels, the inverter, instantaneous examination of alternative energy and storage processes should be done sensitively. In any grid-connected system, an inverter is required to convert direct current to alternating current. Inverter plays a very important role in PVsyst software for design.

Click the 

button. The appropriate inverter is selected from the window that opens, as seen in Figure 12.

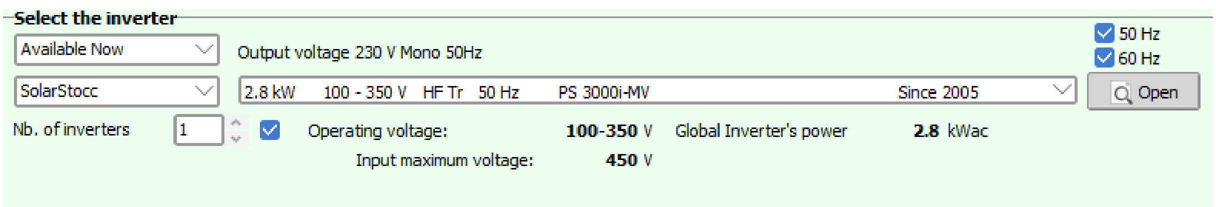

Figure 15. *Inverter Selection Screen*

The efficiency curve of the selected inverter is shown in Figure 13.

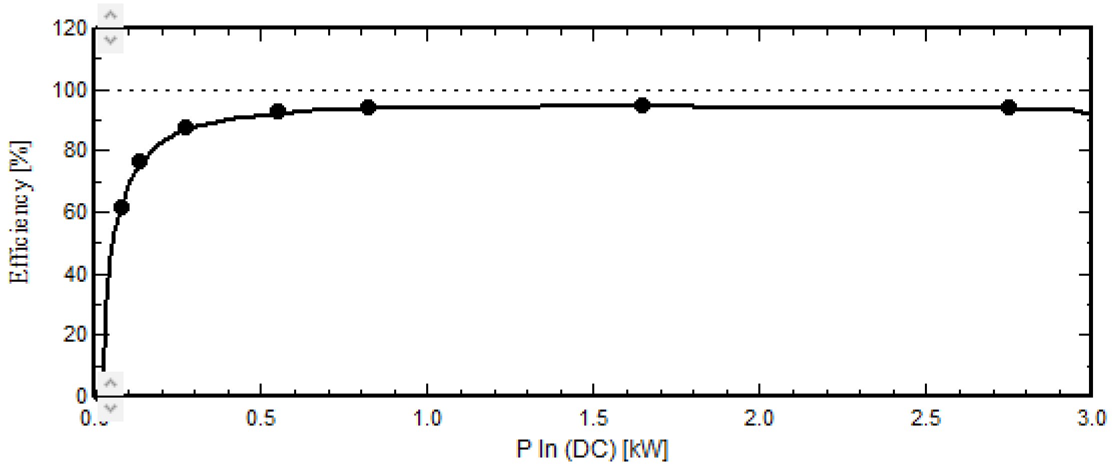

Figure 16. *Efficiency Curve of Inverter*

6.6. Determining the PV Module to be Used in the System

Click the 

button. The appropriate PV module is selected from the window that opens, as seen in Figure 14.

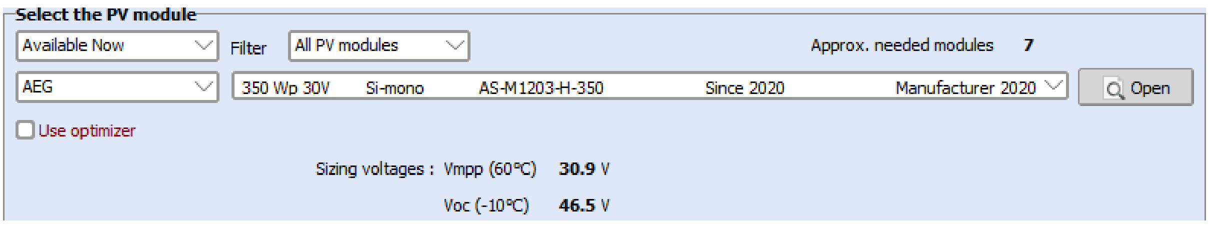

Figure 17. *PV Module Selection Screen*

The features of the selected panel are given in Figure 18 and Figure 19.

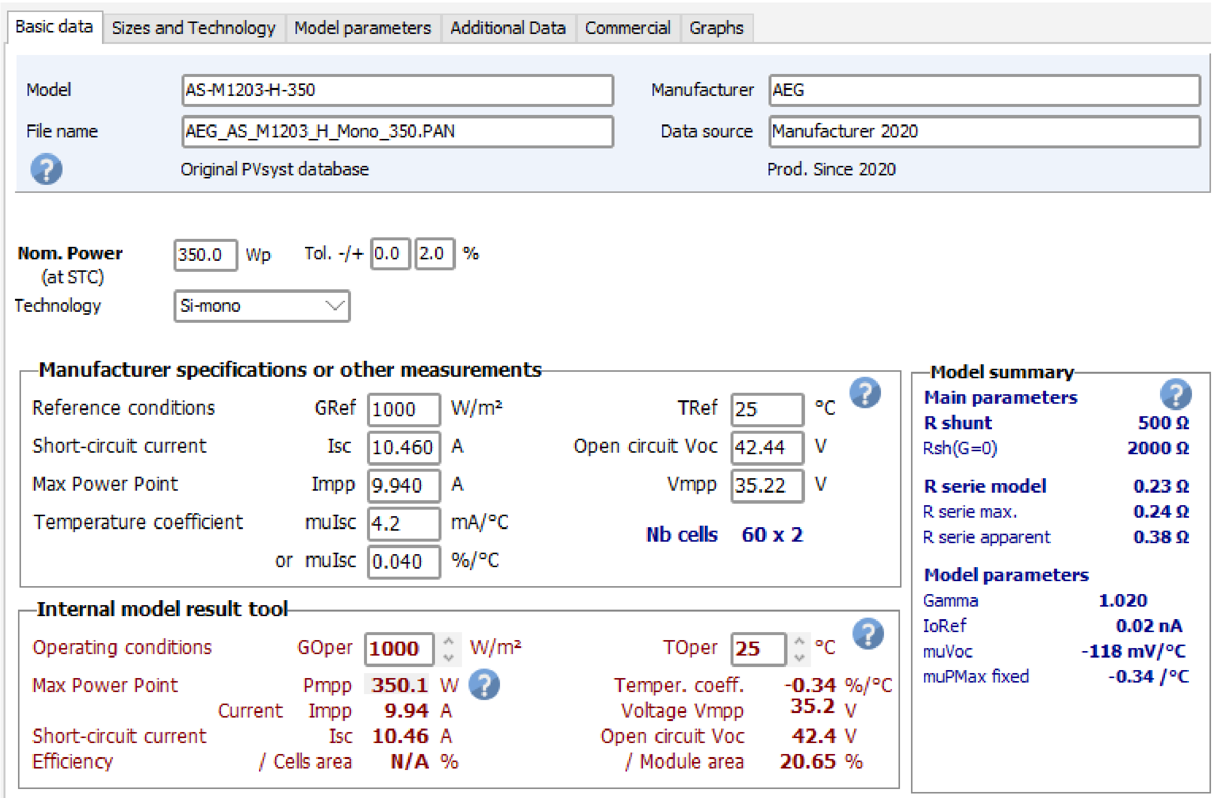

Figure 18. *Panel Features*

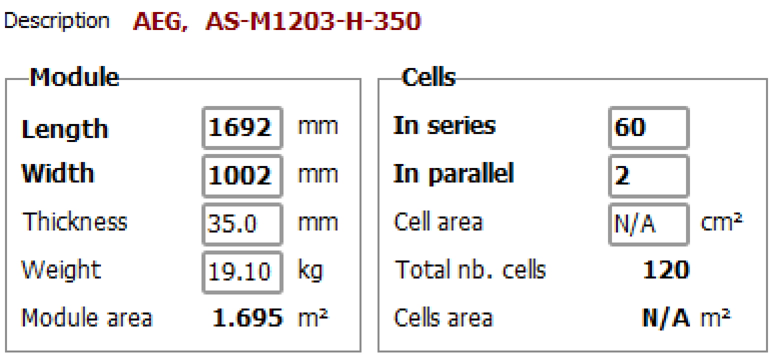

Figure 19. *Panel Features*

Figure 20 shows the PV characteristic curve of the selected module.

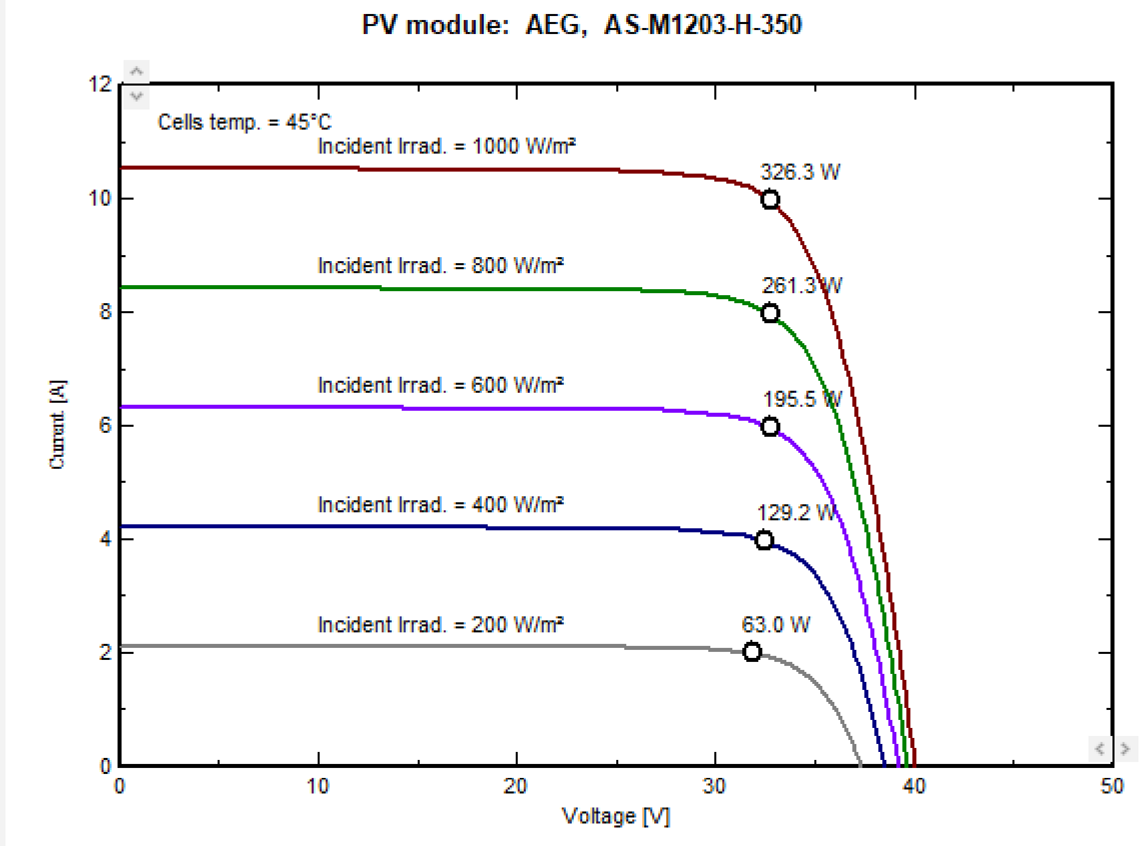

Figure 20. *PV Module Characteristic Curve*

6.7. Horizon Line Diagram

The horizon line is important for solar panel design. Because from here we can see the energy quality of the sun. As can be seen from the figure, while the value is high around 12:00 am at noon, it decreases towards the evening. The azimuth and height values are entered while creating the horizon line. We mentioned earlier in terms of azimuth. The height value is the height of the sun to our position at these different times. [24] is used to get completely real values. As it is shown below when the latitude and longitude values are entered it gives azimuth and corresponding height value. And these values will be used on the PVsyst software for creating a horizon line.

all events of a solar eclipse for: **Mimarsinan, Girne Caddesi 23-23, 16310, Yıldırım, Bursa, TUR**

Latitude: **40.1895°** Height: **164m**
Longitude: **29.1221°** TimeZone: **UTC+3 | local time (without summer time)**

Select Date Range: 2001 - 2100

Calendar Date	Eclipse Type	Partial Eclipse Begins	Sun Alt	A or T Eclipse Begins	Maximum Eclipse	Sun Alt	Sun Azi	A or T Eclipse Ends	Partial Eclipse Ends	Sun Alt	Eclipse Magnitude	Eclipse Observer	A or T Eclipse Duration
31.05.2003	P	05:40(r)	0(r)°	-	06:01:34	03°	064°	-	06:59:11	14°	68.5%	59.3%	-
03.10.2005	P	11:20:03	41°	-	12:40:37	46°	176°	-	14:03:10	43°	50.8%	39.4%	-
29.03.2006	P	12:40:45	53°	-	13:57:21	52°	200°	-	15:12:33	44°	90.7%	89.4%	-
01.08.2008	P	12:41:11	67°	-	13:19:47	68°	186°	-	13:57:34	65°	11.1%	4.4%	-
15.01.2010	P	08:27(r)	0(r)°	-	09:09:34	07°	125°	-	09:58:01	14°	13.7%	5.8%	-
04.01.2011	P	10:07:06	14°	-	11:36:37	24°	157°	-	13:12:08	27°	70.3%	61.5%	-
03.11.2013	P	16:18:24	16°	-	16:40:39	13°	237°	-	17:02:19	09°	4.5%	1.1%	-
20.03.2015	P	11:52:26	46°	-	12:55:58	49°	174°	-	14:00:17	48°	40.9%	29.8%	-
21.06.2020	P	07:51:08	23°	-	08:34:08	31°	085°	-	09:20:11	40°	22.4%	12.3%	-
25.10.2022	P	12:35:39	38°	-	13:48:49	36°	199°	-	15:00:37	29°	48.2%	37.1%	-
02.08.2027	P	11:27:05	58°	-	12:40:01	67°	162°	-	13:52:40	66°	68.6%	62.1%	-
01.06.2030	A	06:53:51	13°	08:01:18	08:02:48	25°	082°	08:04:18	09:21:20	40°	93.8%	88.0%	3m00s
20.03.2034	P	12:47:37	49°	-	13:57:38	48°	198°	-	15:05:34	42°	49.0%	38.4%	-
16.01.2037	P	11:13:26	23°	-	12:45:03	29°	172°	-	14:18:28	27°	50.0%	38.1%	-
05.01.2038	P	17:09:25	06°	-	17:48(s)	0(s)°	240°	-	17:48(s)	0(s)°	43.1%	31.2%	-
02.07.2038	P	17:01:19	38°	-	17:45:43	30°	276°	-	18:27:10	22°	20.2%	10.5%	-
11.06.2048	P	15:59:22	49°	-	17:20:36	34°	273°	-	18:31:16	21°	68.5%	59.3%	-
14.11.2050	P	16:25:53	13°	-	17:36:01	01°	245°	-	17:44(s)	0(s)°	53.1%	41.8%	-
12.09.2053	P	10:29:54	41°	-	11:46:29	50°	151°	-	13:06:38	54°	67.7%	60.1%	-
05.11.2059	P	09:34:35	18°	-	10:56:59	29°	150°	-	12:28:16	34°	70.2%	61.1%	-
30.04.2060	P	12:23:12	64°	-	13:39:46	63°	202°	-	14:56:19	54°	84.8%	82.2%	-
17.02.2064	P	09:16:16	14°	-	09:30:17	16°	122°	-	09:44:16	18°	1.1%	0.1%	-

Figure 21. *Azimuth and Corresponding Height Values[24]*

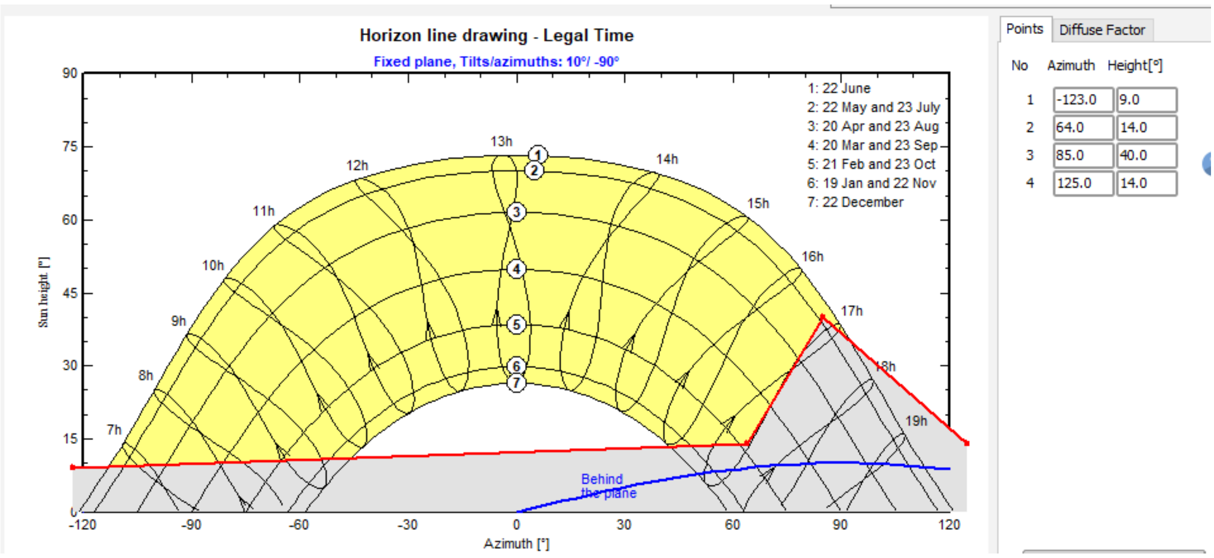

Figure 22. *Horizon Line Diagram*

6.8. PVsyst Simulation Results

Figure 23 is a graphical representation of the performance ratio for each month of the year. The average rate is 0.760.

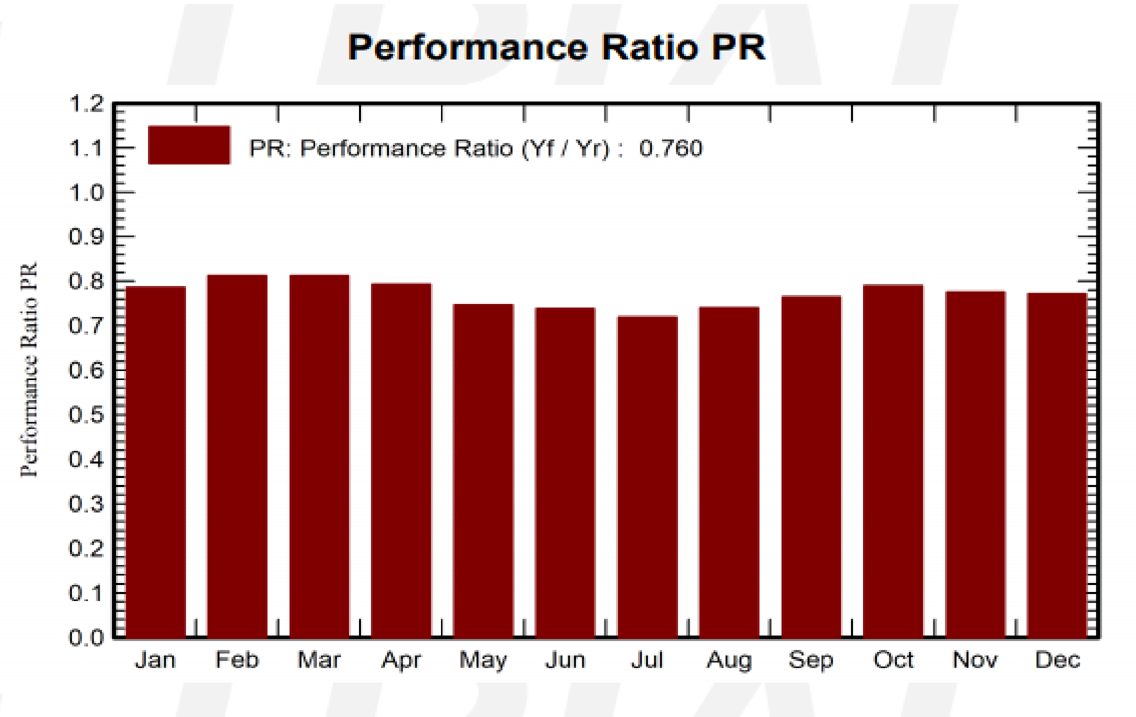

Figure 23. *Monthly Change Graph of Performance Ratio*

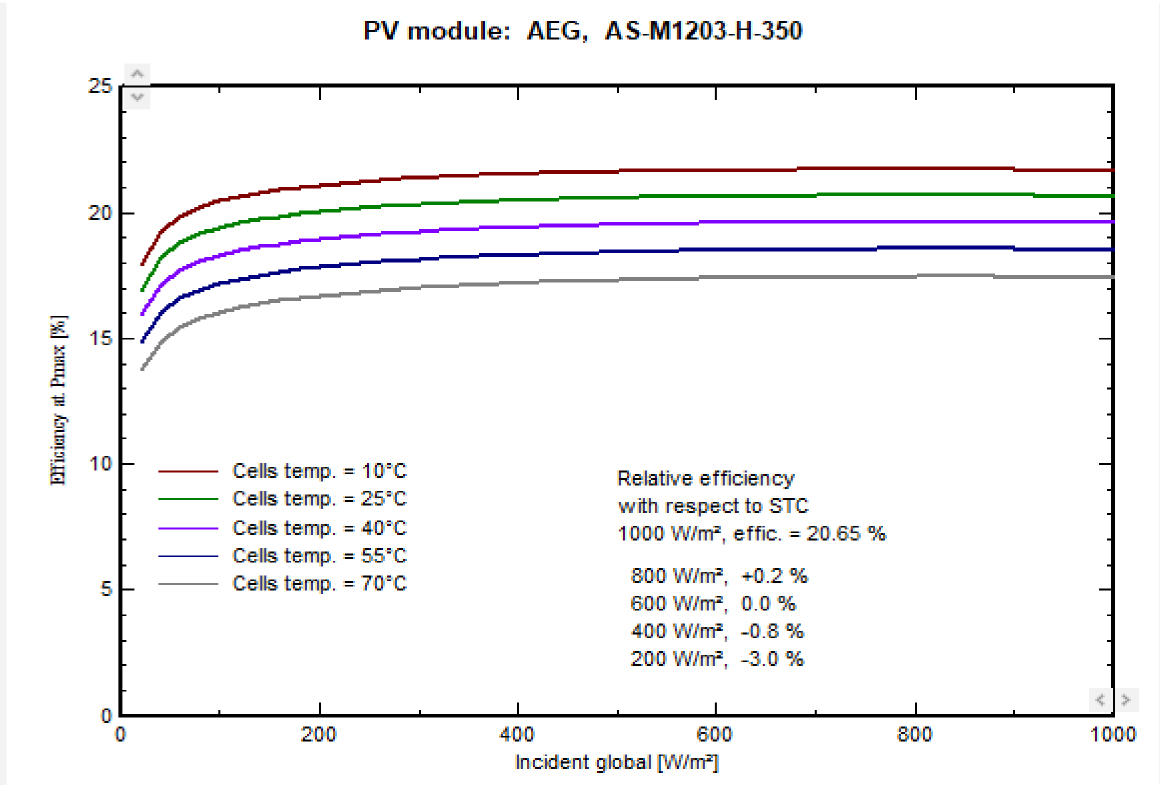

Figure 24. *PV Cell Temperature/Efficiency Graph*

It is clearly seen on Figure 24 that the efficiency of PV cells decreases as a result of the increase in temperature.

Balances and main results

	GlobHor kWh/m²	DiffHor kWh/m²	T_Amb °C	GlobInc kWh/m²	GlobEff kWh/m²	EArray MWh	E_Grid MWh	PR ratio
January	56.5	29.09	5.48	56.0	49.4	0.270	0.247	0.786
February	66.9	41.54	6.99	66.4	60.5	0.328	0.302	0.813
March	109.3	59.51	10.00	108.6	99.9	0.531	0.494	0.812
April	147.5	74.38	13.45	146.4	133.9	0.697	0.650	0.793
May	195.5	75.34	18.98	194.5	173.5	0.873	0.813	0.747
June	211.7	80.49	23.24	210.4	188.3	0.930	0.869	0.737
July	217.9	76.01	26.57	216.7	192.5	0.935	0.873	0.719
August	190.4	72.37	26.58	189.4	171.8	0.840	0.785	0.740
September	142.5	57.77	21.45	141.8	129.3	0.651	0.607	0.764
October	93.0	46.68	16.27	92.3	84.6	0.440	0.408	0.789
November	62.6	33.47	11.33	62.1	55.0	0.294	0.270	0.775
December	48.4	27.73	7.04	47.8	41.8	0.227	0.207	0.771
Year	1542.2	674.38	15.67	1532.4	1380.5	7.016	6.524	0.760

Legends

GlobHor	Global horizontal irradiation
DiffHor	Horizontal diffuse irradiation
T_Amb	Ambient Temperature
GlobInc	Global incident in coll. plane
GlobEff	Effective Global, corr. for IAM and shadings
EArray	Effective energy at the output of the array
E_Grid	Energy injected into grid
PR	Performance Ratio

Figure 25. *General Results*

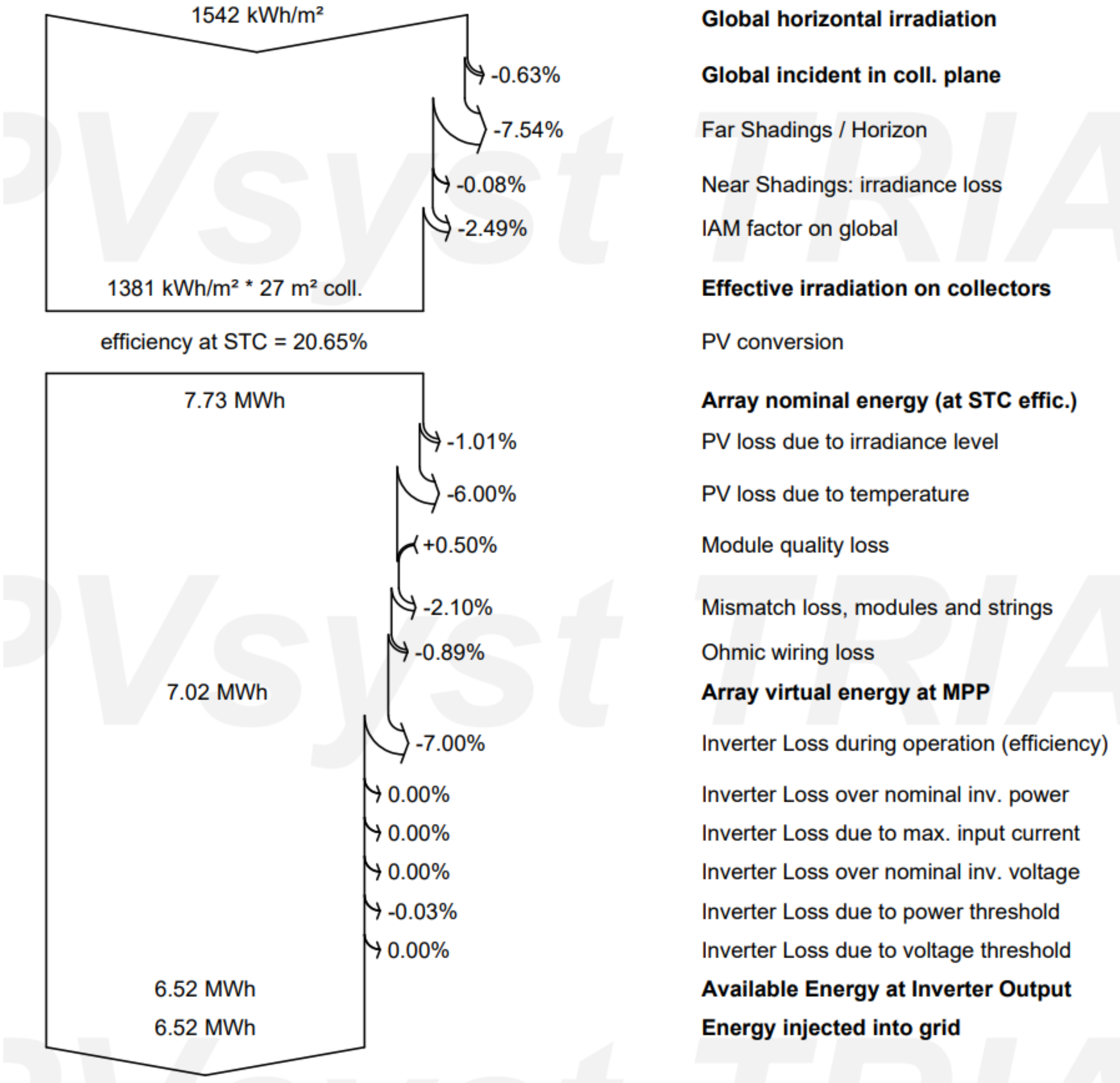

Figure 26. *Loss Diagram for The Whole Year*

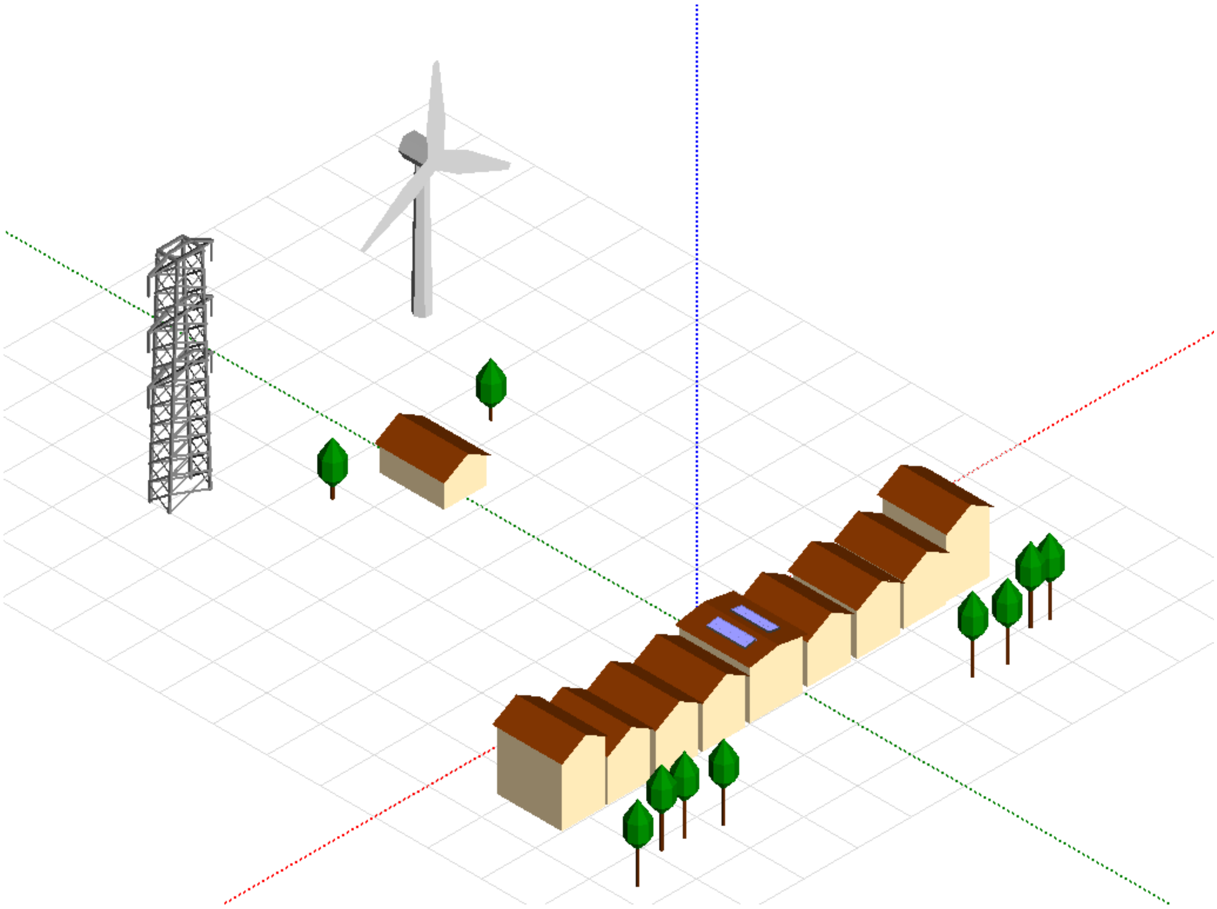

Figure 27. *Shading Scene Construction*

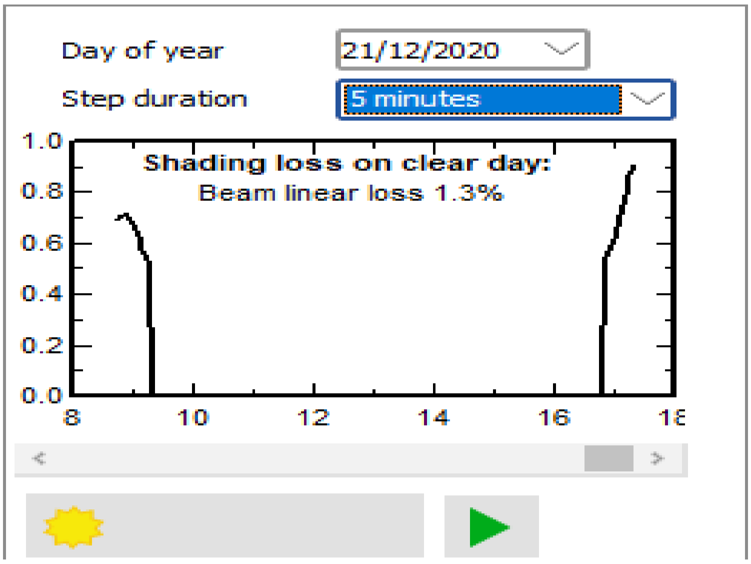

Figure 28. *Shading Loss*

7. PVSYST MODULE PERFORMANCE MODEL

After examining the working principle of the PVsyst program, it will now be examined the equations that are used to obtain these results and graphics.

Popular PVsyst software for modelling photovoltaic system performance uses a single diode model to calculate the I-V curve for a module or array of modules at a given irradiance and temperature conditions. A single diode model requires a set of parameters to be estimated, preferably from the measured I-V curves. Many existing parameter estimation methods use only short-circuit, open-circuit, and maximum power points for a single I-V curve under standard test conditions and temperature coefficients determined from testing individual cells.[28]

Now, some techniques will be adapted to present an algorithm to determine the parameters for the photovoltaic module performance model encoded in the PVsyst software. The diode model which is encoded in the PVsyst software predicts the module current I and voltage V as a function of the module-averaged cell temperature T_C and the effective irradiance E.The module performance model in the PVsyst software comprises the single diode equation as given below. [28]

$$I = I_L - I_O\left[\exp\left(\frac{V + IR_S}{\gamma V_{th}}\right) - 1\right] - \left(\frac{V + IR_S}{R_{SH}}\right) \tag{1}$$

together with the following equations; [28]

The photo-generated current is calculated by 2 as seen in below.

$$I_L = I_L\left(E, T_C\right) = \frac{E}{E_0}\left[I_{L0} + \alpha_{ISC}\left(T_C - T_0\right)\right] \tag{2}$$

The dark saturation current is calculated by Eq. (3).

$$I_O = I_O\left(T_C\right) = \left[\frac{T_C}{T_0}\right]^3 \exp\left[\frac{q\varepsilon_G}{K\gamma}\left(\frac{1}{T_0} - \frac{1}{T_C}\right)\right] \tag{3}$$

The diode ideality factor can be found by using Eq. (4)

$$\gamma = \gamma_0 + \mu_{\gamma}\left(T_C - T_0\right) \tag{4}$$

And then shunt resistance can be calculated as shown below

$$R_{SH} = R_{SH,base} + \left(R_{SH,0} - R_{SH,base}\right)\exp\left(-R_{SH\exp}\frac{E}{E_0}\right) \tag{5}$$

The shunt resistance in the absence of irradiance calculated as given in Eq. (6)

$$R_{SH,base} = \max\left[\frac{R_{SH,ref} - R_{SH,0}\exp\left(-R_{SH\exp}\right)}{1-\exp\left(-R_{SH\exp}\right)}\right] \tag{6}$$

$$R_S = R_{S0} \tag{7}$$

7.1. Data Methodology for PVsyst

Data required for estimation of parameters fall into two categories; determining temperature coefficients and the estimation of other parameters.

To determine the temperature coefficients, we assume that the I-V curves are measured outdoors with an air mass close to 1.5 and the angle of incidence of zero, or indoors using a flash tester calibrated to these conditions. Simultaneously with the I-V curves, the mean(average) cell temperature T_C should be measured or estimated and the plane of array irradiation measured. Cell temperature is often estimated from measurements of the back-surface temperature of the module. Plane of array radiation for temperature coefficient determination should be kept around 1000 W/m^2 when changing module temperature; Usually the 25°C range is sufficient.

Step 1: Temperature coefficients determination :

The change in I_{SC} with temperature as given below [28]

$$I_{SC} = \frac{E}{E_0}\left(I_{SC0} + \alpha_{ISC}(T_C - T_0)\right) \tag{8}$$

where α_{ISC} and I_{SC0} are unknown terms. It can be rearranged to obtain

$$\begin{aligned} I_{SC}\frac{E_0}{E} &= \left(I_{SC0} + \alpha_{ISC}(T_C - T_0)\right) \\ &= \beta_0 + \beta_1(T_C - T_0) \end{aligned} \tag{9}$$

By using measured T_C, I_{SC} and E values, obtain coefficients β_0, β_1 from α_{ISC} is determined:[28]

$$\alpha_{ISC} = \beta_1 \tag{10}$$

Step 2: Diode factor terms determinations:

Step 2a: Estimation of initial value for R_{SH}

For every I-V, initial value for R_{SH} will be determined with regression involving co-content (CC). The co-content is exactly equal to a polynomial in V and $I = I(V)$ [28]

$$CC(V) = \int_0^V \left(I_{SC} - I(v)\right)dv = c_1 V + c_2(I_{SC} - I) + c_3 V(I_{SC} - I) + c_4 V^2 + c_5(I_{SC} - I)^2 \tag{11}$$

Using the equation given above R_{SH} is determined as

$$R_{SH} = 1/2c_4 \tag{12}$$

where the constant c_4 found by regression.

Step 2b: Estimation of temperature coefficient μ_γ, and diode factor γ_0

These parameters are estimated by a linear regression:

$$\begin{aligned}\ln\left(I_{SC} - \frac{V_{OC}}{R_{SH}}\right) - 3\ln\left(\frac{T_C}{T_0}\right) = c_1 + c_2\frac{q}{k}\left(\frac{1}{T_C} - \frac{1}{T_0}\right) - c_3\frac{q}{k}\left(\frac{1}{T_C} - \frac{1}{T_0}\right) \\ + c_4\frac{V_{OC}}{V_{th}} - c_5\frac{V_{OC}}{V_{th}}\left(T_C - T_0\right)\end{aligned} \tag{13}$$

where
$$\gamma_0 = \frac{1}{c_4} \tag{14}$$

$$\mu_\gamma = c_5 {\gamma_0}^2 \tag{15}$$

Eq. (13) combining from Eq. (1) with Eq. (3) along with several approximations. At I_{SC} from Eq. (1) we obtain [28]

$$I_{SC} = I_L + I_0 - I_0 \exp\left(\frac{I_{SC}R_S}{\gamma V_{th}}\right) - \frac{I_{SC}R_S}{R_{SH}} \tag{16}$$

and from Eq. (1) at V_{OC}

$$0 = I_L + I_0 - I_0 \exp\left(\frac{V_{OC}}{\gamma V_{th}}\right) - \frac{V_{OC}}{R_{SH}} \tag{17}$$

Subtracting Eq. (17) from Eq. (16)

$$
\begin{aligned}
I_{SC} &= I_0 \exp\left(\frac{V_{OC}}{\gamma V_{th}}\right) - I_0 \exp\left(\frac{I_{SC} R_S}{\gamma V_{th}}\right) + \frac{V_{OC} - I_{SC} R_S}{R_{SH}} \\
&\approx I_0 \exp\left(\frac{V_{OC}}{\gamma V_{th}}\right) + \frac{V_{OC} - I_{SC} R_S}{R_{SH}}
\end{aligned} \tag{18}
$$

where the approximation is justified generally because $R_S < 1\Omega$, $I_{SC} < 10A$, $I_0 < 10^{-7}$ and $\gamma V_{th} \approx 2V$ so $I_0 \exp\left(I_{SC} R_S / \gamma V_{th}\right) < 10^{-7} \exp(5) \approx 1.5*10^{-5}$. Solving Eq. (18) for I_{SC} and approximating $\frac{R_{SH}}{R_{SH} + R_S} \approx 1$ [28]

$$
\begin{aligned}
I_{SC} &\approx \frac{R_{SH}}{R_{SH} + R_S}\left[\frac{V_{OC}}{R_{SH}} + I_0 \exp\left(\frac{V_{OC}}{\gamma V_{th}}\right)\right] \\
&\approx \frac{V_{OC}}{R_{SH}} + I_0 \exp\left(\frac{V_{OC}}{\gamma V_{th}}\right)
\end{aligned} \tag{19}
$$

substituting Eq. (3) and applying a logarithm creates [28]

$$
\ln\left(I_{SC} - \frac{V_{OC}}{R_{SH}}\right) \approx \ln I_{O0} + 3\ln\left(\frac{T_C}{T_0}\right) + \frac{q\varepsilon_G}{k\gamma}\left(\frac{1}{T_0} - \frac{1}{T_C}\right) + \frac{V_{OC}}{\gamma V_{th}} \tag{20}
$$

From Eq. (4) and the general assumption that $\frac{\mu_\gamma}{\gamma_0}\left(T_C - T_0\right) \ll 1$ it is approximated [28]

$$
\begin{aligned}
\frac{1}{\gamma} &= \frac{1}{\gamma_0 + \mu_\gamma\left(T_C - T_0\right)} = \frac{1}{\gamma_0} \frac{1}{1 + \frac{\mu_\gamma}{\gamma_0}\left(T_C - T_0\right)} \\
&\approx \frac{1}{\gamma_0}\left(1 - \frac{\mu_\gamma}{\gamma_0}\left(T_C - T_0\right)\right) = \frac{1}{\gamma_0} - \frac{\mu_\gamma}{\gamma_0^{\ 2}}\left(T_C - T_0\right)
\end{aligned} \tag{21}
$$

Substituting Eq. (21) into Eq. (20) and rearranging obtains [28]

$$
\begin{aligned}
\ln\left(I_{SC} - \frac{V_{OC}}{R_{SH}}\right) - 3\ln\left(\frac{T_C}{T_0}\right) &\approx \ln I_{O0} + \frac{\varepsilon_G}{\gamma_0}\frac{q}{k}\left(\frac{1}{T_0} - \frac{1}{T_C}\right) - \frac{\varepsilon_G \mu_\gamma}{\gamma_0^{\ 2}}\frac{q}{k}\left(\frac{1}{T_0} - \frac{1}{T_C}\right)\left(T_C - T_0\right) \\
&\quad + \frac{1}{\gamma_0}\frac{V_{OC}}{V_{th}} - \frac{\mu_\gamma}{\gamma_0^{\ 2}}\frac{V_{OC}}{V_{th}}\left(T_C - T_0\right)
\end{aligned} \tag{22}
$$

which is in the form of Eq. (13), with all the terms on the left-hand side are known from measurements, and the unknown terms that are on the right-hand side comprising $\varepsilon_G / \gamma_0, \ln I_{O0}, \varepsilon_G \mu_\gamma / \gamma_0^2, 1/\gamma_0, \mu_\gamma / \gamma_0^2$. μ_γ and γ_0 are determined as indicated in Eq. (14) and Eq. (15).

Step 3a: Find initial values for R_S, I_L and I_0.

The estimate of I_0 is obtained from Eq. (19) [28]:

$$I_0 = \left(I_{SC} - \frac{V_{OC}}{R_{SH}} \right) \exp\left(-\frac{V_{OC}}{\gamma V_{th}} \right) \tag{23}$$

With a value for I_0 in left hand, the first estimation of R_S is obtained from the slope of the I-V curve near V_{OC} (but not *at* V_{OC}). And the derivative $\frac{dI}{dV}$ will be negative and smoothly decreasing as $V \to V_{OC}$. Estimation of the derivative from data requires use of some kind of numeric differentiation scheme. For measured I-V curves it cannot be assumed that the points comprising the I-V curve are taken at equally spaced voltage values and eventually most common finite difference approximations are not suitable. A fifth-order finite difference technique with unequally spaced data will be used to estimate. [28]

$$I_V'(V_k) = \left. \frac{dI}{dV} \right|_{V=V_k}, k = 1, \ldots, M \tag{24}$$

for data at voltages V_k where $L = 0.5V_{OC} < V_k < 0.9V_{OC} = R$ and $k = 1, \ldots, M$. Then R_S can be estimated as the average (Eq. (25))

$$R_S \cong \frac{1}{M} \sum_{k=1}^{M} R_{S,k} \tag{25}$$

where

$$R_{S,k} = \frac{\gamma V_{th}}{I_{SC}} \left[\ln\left(-\left(R_{SH} I_V'(V_k) + 1 \right) \frac{\gamma V_{th}}{R_{SH} I_0} \right) - \frac{V_k}{\gamma V_{th}} \right] \tag{26}$$

for points where $R_{SH} I_V'(V_k) + 1 < 0$. Finally, I_L is estimated by evaluating Eq. (1) at I_{SC} :

$$I_L = I_{SC} - I_0 + I_0 \exp\left(\frac{R_S I_{SC}}{\gamma V_{th}} \right) + \frac{R_S I_{SC}}{R_{SH}} \tag{27}$$

Step 4: Obtain parameter values for the PVsyst single diode model

A value for I_{L0} is obtained by rearranging Eq. (2) as; [28]

$$I_{L0} = I_L \frac{E_0}{E} - \alpha_{Isc}\left(T_C - T_0\right) \quad (28)$$

and estimate I_{L0} as the average value of the right-hand side of Eq. (28) over all I-V curves. And then I_{O0}, ε_G can be estimated from Eq. (3) by re-arranging as

$$\ln\left(I_O\right) - 3\ln\left(\frac{T_C}{T_0}\right) = \ln I_{O0} + \frac{q}{k\gamma}\left(\frac{1}{T_0} - \frac{1}{T_C}\right)\varepsilon_G \quad (29)$$

and by regressing $\ln\left(I_O\right) - 3\ln\left(\frac{T_C}{T_0}\right)$ onto $\frac{q}{k\gamma}\left(\frac{1}{T_0} - \frac{1}{T_C}\right)$. And values for $R_{SH,0}$, $R_{SH,ref}$ and $R_{SH,\exp}$ are determined by nonlinear minimization. The equation relating R_{SH} to effective irradiance *E* (Eq. (30) and Eq. (31)) are defined piecewise and are nonlinear.

$$R_{SH} = R_{SH,base} + \left(R_{SH,0} - R_{SH,base}\right)\exp\left(-R_{SH\exp}\frac{E}{E_0}\right) \quad (30)$$

$$R_{SH,base} = \max\left[\frac{R_{SH,ref} - R_{SH,0}\exp\left(-R_{\mathrm{SH\ exp}}\right)}{1 - \exp\left(-R_{\mathrm{SH\ exp}}\right)}, 0\right] \quad (31)$$

Eventually when determined jointly the optimum values for $R_{SH,0}$, $R_{\mathrm{SH\ exp}}$, $R_{SH,ref}$ are highly sensitive to minor variations in the data. For this reason, it can be elected to fix $R_{\mathrm{SH\ exp}} = 5.5$ at the PVsyst default value, because the parameters $R_{SH,0}$ and $R_{SH,ref}$ appear to be less sensitive to large variation in the values for R_{SH}, and also to use a logarithm to reduce the influence of extreme values for R_{SH}. [28]

$R_{SH,ref}$ and $R_{SH,0}$ will be determined by minimizing

$$C\left(R_{SH}\left(R_{SH,ref}, R_{SH,0}\right)\right)\sum\left(\log_{10} R_{SH}\left(R_{SH,ref}, R_{SH,0}\right) - \log_{10} R_{SH}\right)^2 \quad (32)$$

where $R_{SH}\left(R_{SH,ref}, R_{SH,0}\right)$ is computed as indicated in Eq. (30) and Eq. (31) with $R_{\mathrm{SH\ exp}} = 5.5$ R_{SH} is the value determined for a measured I-V curve and the summation is over all measured I-V curves. [28]

All the equations given above are to summarize the working logic of the PVsyst program. As can be seen above, only equations and usage patterns are explained. In order not to go into too much detail, manual calculations for the Bursa project will not be made using the above equations. But as can be seen from the simple energy equation given Eq.33, the program gives correct results.

7.2. Manuel Energy Calculation for Comparison

The electrical energy (E) produced in the PV system is determined by the equation which is given below.[25]

$$E = A * \eta * I_T * Pr \qquad (33)$$

where ;

E = Energy (kWh),

A = Total solar panel Area (m^2),

η = solar panel efficiency(%) ,

I_T =solar radiation on tilted panels,

Pr =Performance ratio, coefficient for losses (range between 0.5 and 0.9)

$E = A * \eta * I_T * Pr$= (27 m^2) *(0.2065)*(1542.2 kWh/ m^2)*(0.760)=6534.88 kWh

As it seen in the equation calculated above, the value in the software program (6.52 MWh) and the equation value calculated manually (6.535 MWh) are quite close to each other. Thus, we conclude that the PVsyst program we used for solar panel design is applicable.

8. ECONOMIC ANALYSIS OF THE SYSTEM

The most important part of a power plant for the investor is the economic analysis of the investment he will make and knowing when the financial fee he has invested will return to him and start to make a profit. For this reason, the calculations should be made to inform the repayment plans and to explain the value of the investment.

The stages required for the installation of the solar power plant, knowing the material and hardware values, are the subjects required to be able to analyse it. The most important factor in the analysis is to understand whether the investment is necessary. In projects that are expected to generate income, it is very important for the investor to see how much they will earn during the project.

Economic aspects should also be considered to evaluate the benefits of investment in PV power systems. Among the different measures of the economic value of an investment, such as life cycle cost (LCC), levelized cost of energy (LCOE), and payback period, a proper economic analysis can guarantee the profitability of the investment in PV systems.

In this design, the costs of all parameters to be used for installation are entered into the PVsyst program and the initial installation cost is calculated.

The first step of the economic evaluation consists in defining investment costs and charges.

The initial investment costs of the system will be defined as seen in figures 29 and 30. Investment consists of component costs, other costs such as studies, installation, insurance, and taxes.

Some quantities for components are retrieved from the system definitions, they cannot be modified.

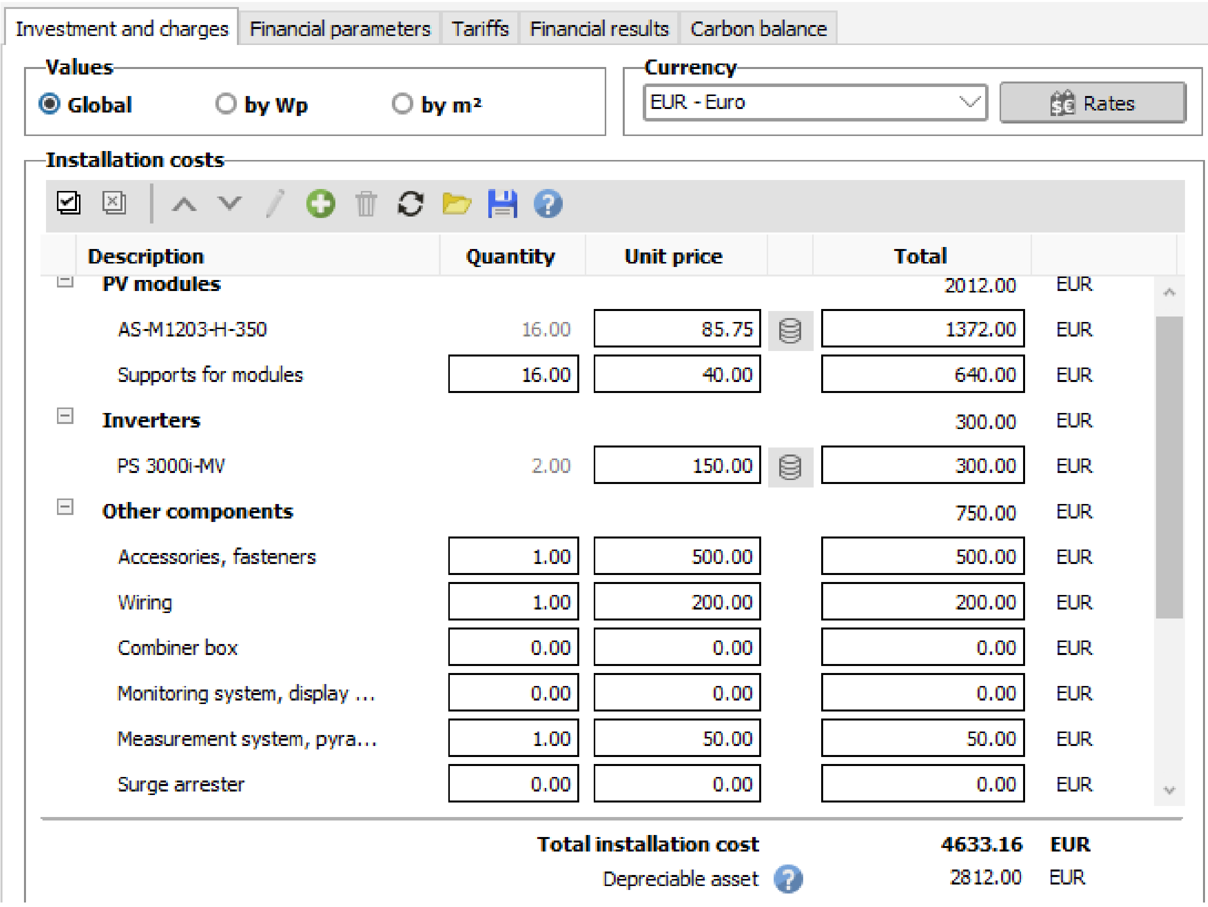

Figure 29. *Investment Costs*

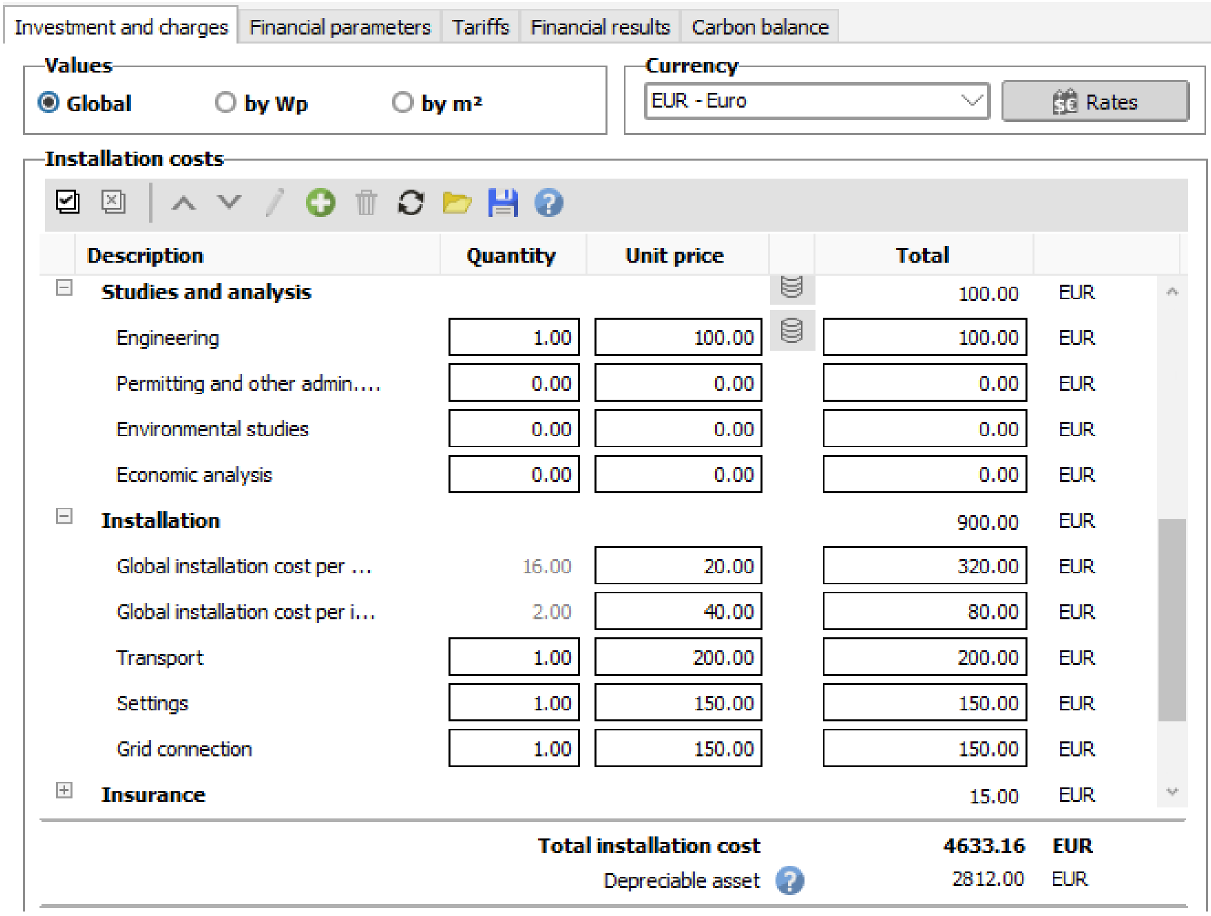

Figure 30. *Investment Costs*

Then the yearly operation costs, such as maintenance, salaries, cleaning, security fund, and taxes. But in this design the salaries, , cleaning, and security fund will be ignored because it's just small roof-top PV system.

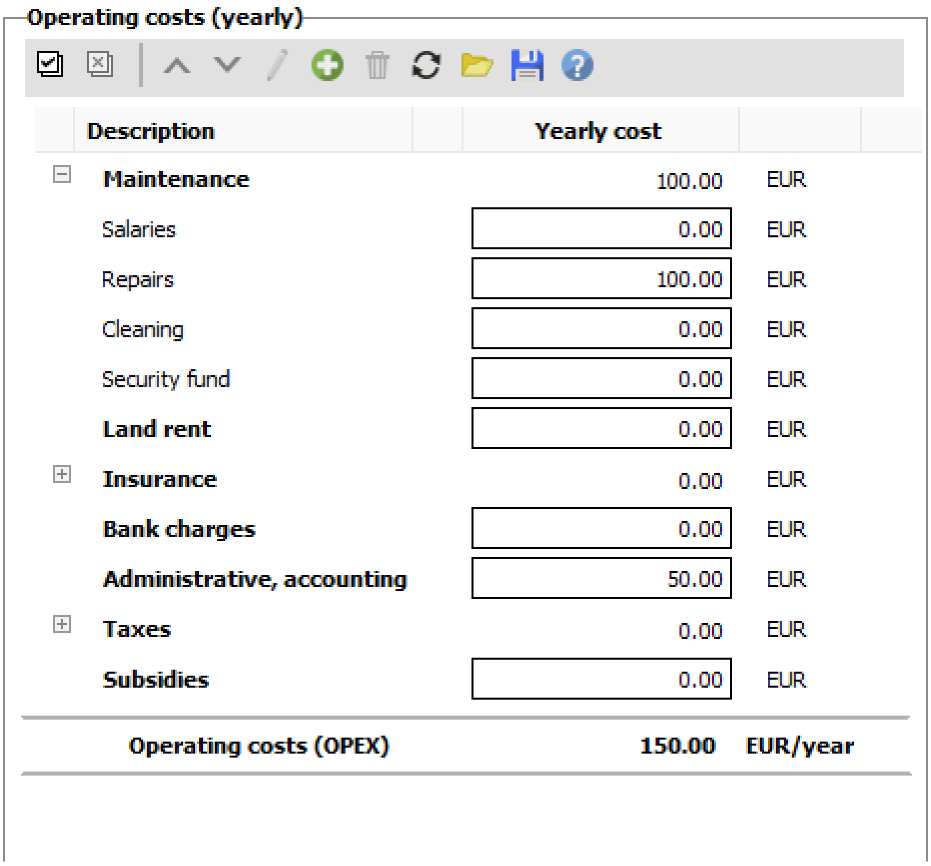

Figure 31. *Operating Costs*

After completing operating costs, then the financial parameters will be defined on the program.

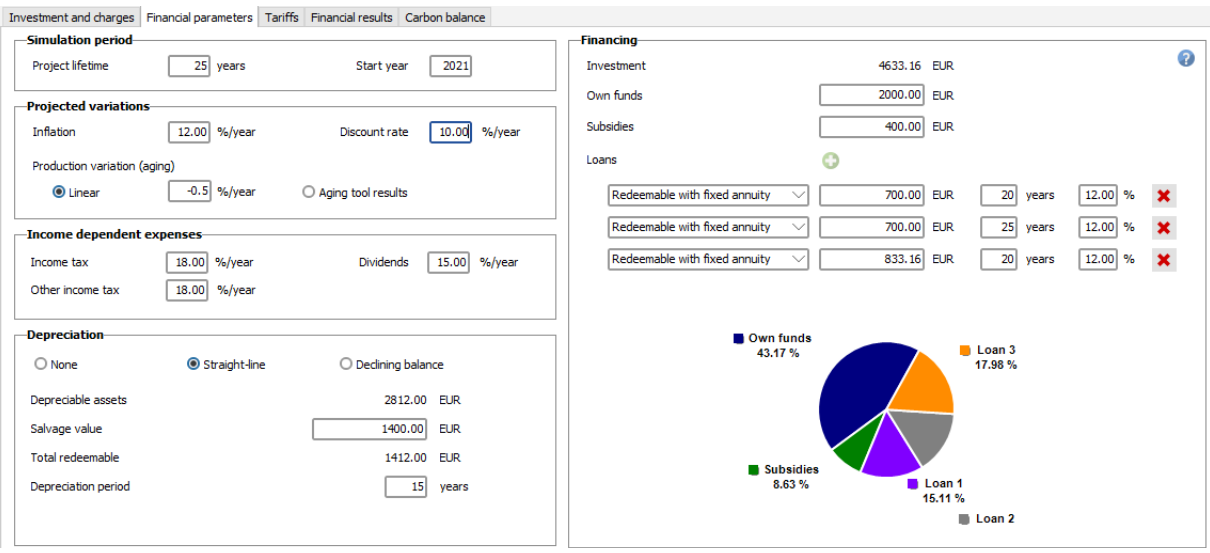

Figure 32. *Financial Parameters*

8.1. Techno-Economic Feasibility Analysis

This part investigates the techno-economic feasibility of installing a 5-kilowatt peak (kWp) PV system in Bursa, Turkey. The technical viability of the PV system is evaluated using PVsyst and Meteonorm simulation software tool. The performance indicators adopted in our study are the performance ratio, electric energy output, economic returns including the levelized cost and the net present value of energy production of the design. The key parameters used in simulations are solar irradiance, site-specific meteorological data etc...

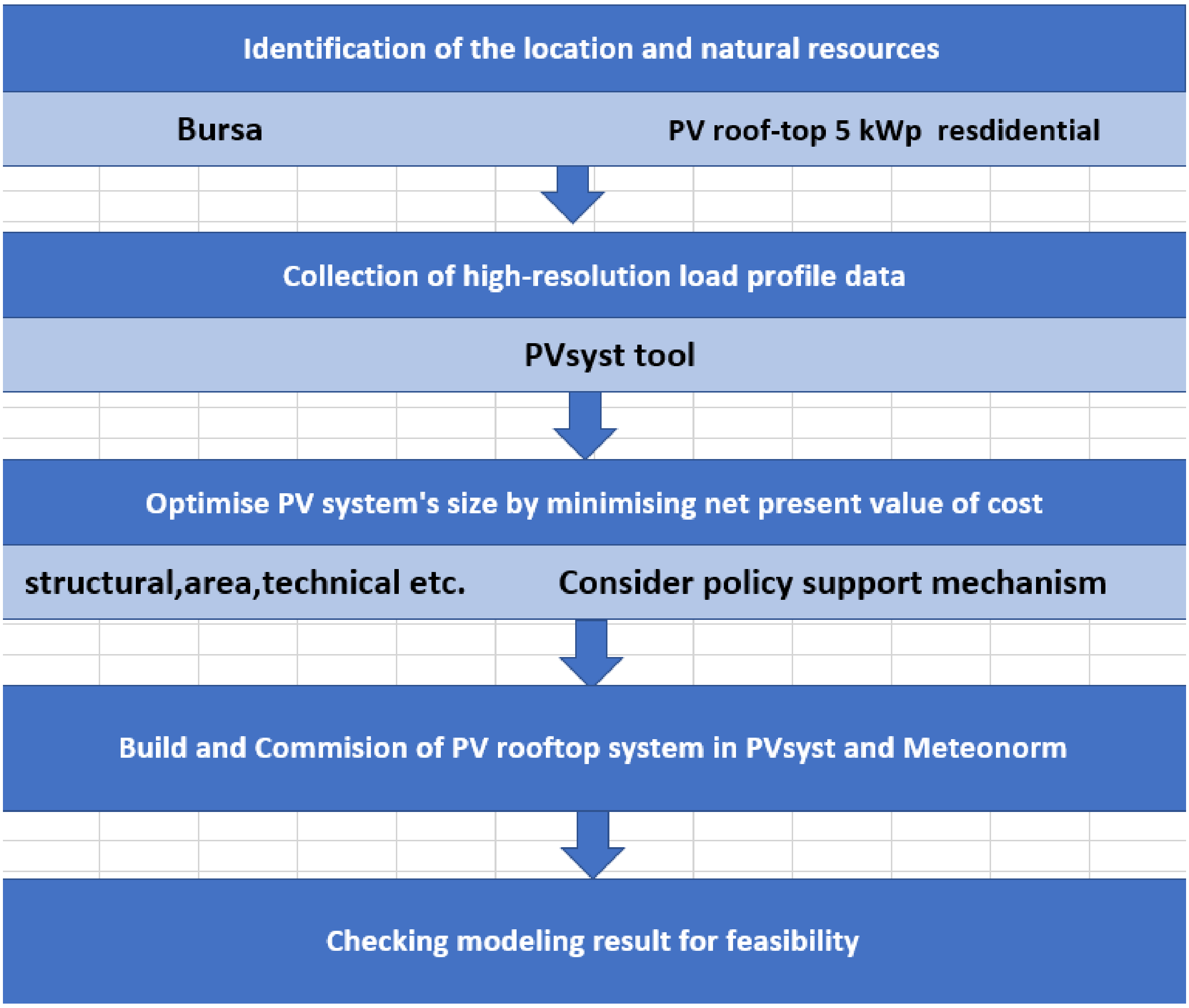

Figure 33. *A Flowchart Summarizing Our Techno-Economic Evaluation Methodology*

The detailed economic results show that the total yearly cost, including 12 inflation per year, is €1053.46/year, with a produced energy of 6.52 MWh/year, and the cost of the production is €0.197 per kWh. The payback period is 9.6 years, and the return on investment (ROI) is 39.7%.

Moreover, projections indicate that the design may be feasible if the declining trend in PV system prices continues and electricity prices continue to increase in Turkey. The payback period for the grid-connected system is 9.6 years and the return on investment (ROI) is 39.7%. Therefore, it can be said that the system is techno-economically viable.

9. STRUCTURAL ANALYSIS OF THE ROOF FOR SOLAR PANEL DESIGN

Structural failures occur when a structure or structural member loses or potentially deteriorates its ability to carry a load. Common examples of failures include excessive deflection in a structural joist or overhanging roof, insufficient connection strength, splitting of the chord of a timber joist, or a roof penetration causing a roof leak that could result in failure of a structural member. This section aims to help installers properly evaluate and analyse support structures for solar equipment installation. If the structural load analysis is not taken into account when designing the solar panel, catastrophic accidents can occur as seen in Figures 34 and 35.

Figure 34. *Roof Collapse Due to Excessive Snow Load [26]*

Figure 35. *Truss Failure Due to Excessive Roof Load [26]*

To avoid failure, solar installers should not exceed the maximum bearing capacity of the structure with a solar system installation. Stability failures and strength failures are two types of structural failures that are relevant to solar installers:

- Strength fractures are related to the parts that make up a structure.
- Stability failures are related to the structural systems.

Strength failures include overbending, horizontal shear, and vertical shear. Bending is the most common type of strength loss as seen in figure 36. A failure due to bending can occur when the applied stresses exceed the allowable bending strength of the members of the structure or when the resulting deflection exceeds the allowable deflection in that member. When a simple beam is loaded in bending, the top is compressed and the bottom is in tension. If the beams are not supported in the lateral direction, and the bending load rises to a critical limit, the beams will fail due to lateral buckling of the compression flange. In large-flanged sections, if the compression flange is bent laterally, the cross-section will also twist in torsion, resulting in a failure mode known as lateral-torsional buckling.

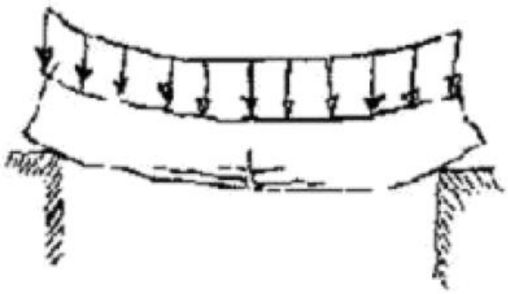

Figure 36. *Bending in the Beam [26]*

Failures of stability are usually related to structural systems. These failures may be caused by lateral loads from seismic events or wind. Examples for individual members include:

- Columns fail because of elastic instability (i.e., column buckling)
- Beams fail because of lateral or lateral-torsional buckling

Elastic instability causes a member to buckle as seen in figure 37. It is characterized by a sudden failure of a structural element that is subjected to high compressive stresses. The actual compressive stress at the breaking point is less than the ultimate compressive stresses of that material. If the load applied to a column passes through the center of gravity of its section, it is defined as axial load. The eccentric load on a column or pile that is not symmetrical about the central axis creates a bending moment in addition to the axial load. Eccentric loads promote buckling at lower compressive stress due to the induced couple.

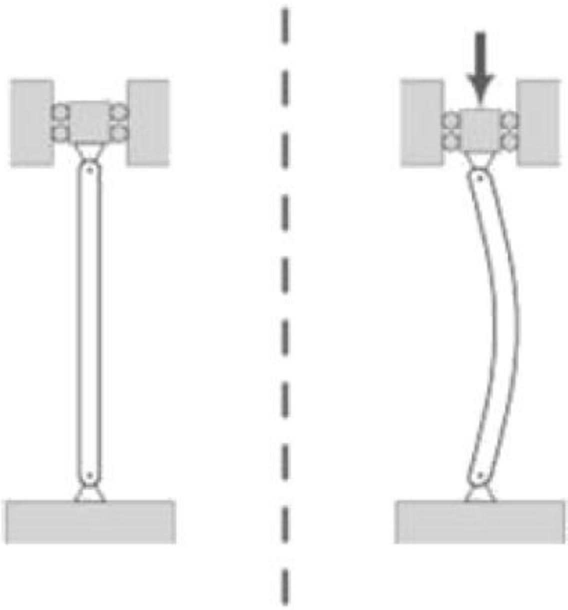

Figure 37. *Axial Load in the Column [26]*

9.1. Assessment of the Roof Structure

Before installing a rooftop solar system, the condition of the roof structure should be evaluated. This assessment should consider whether the existing structure has excess capacity for additional loads due to the solar installation or whether modifications are required for the installation of solar panels. The condition of rafters, size, and spacing should be assessed before the solar energy system installation. The roof trusses are an assembly of pieces that are connected by steel plates to form a unified structural member. It is important to understand that each member of a truss is essential for adequate performance. Therefore, any repair, modification, or damage to a truss member affects the entire truss and its ability to resist the loads placed on it. If a truss member is cut or removed, the entire truss will fail unless remedial work is done to properly redistribute the loads around the modified portion of the truss.

Load types on the building structures are shown below. [27]

Vertical Loads

- Dead (gravity)
- Live (gravity)
- Snow (gravity)
- Wind (uplift on the roof)
- Seismic and wind (overturning)
- Seismic (vertical ground motion)

Horizontal (Lateral) Loads

- Wind
- Seismic (horizontal ground motion)
- Flood (static and dynamic hydraulic forces)
- Soil (active lateral pressure)
- Tsunami (dynamic hydraulic and forces)

Loads generate stresses on various systems, elements, and connections. The path through which the loads are transferred is known as the load path. A continuous load path is capable of resisting and transferring loads performed throughout the structure from the load origin to the foundation. Figures 38 and 39 show vertically oriented loads created, respectively, by wind uplift and gravity. The wind uplift load results from suction forces acting on the roof perpendicular to the outer surface of the roof, as well as internal pressure acting vertically outward on the inner surface of the roof-ceiling assembly. [27]

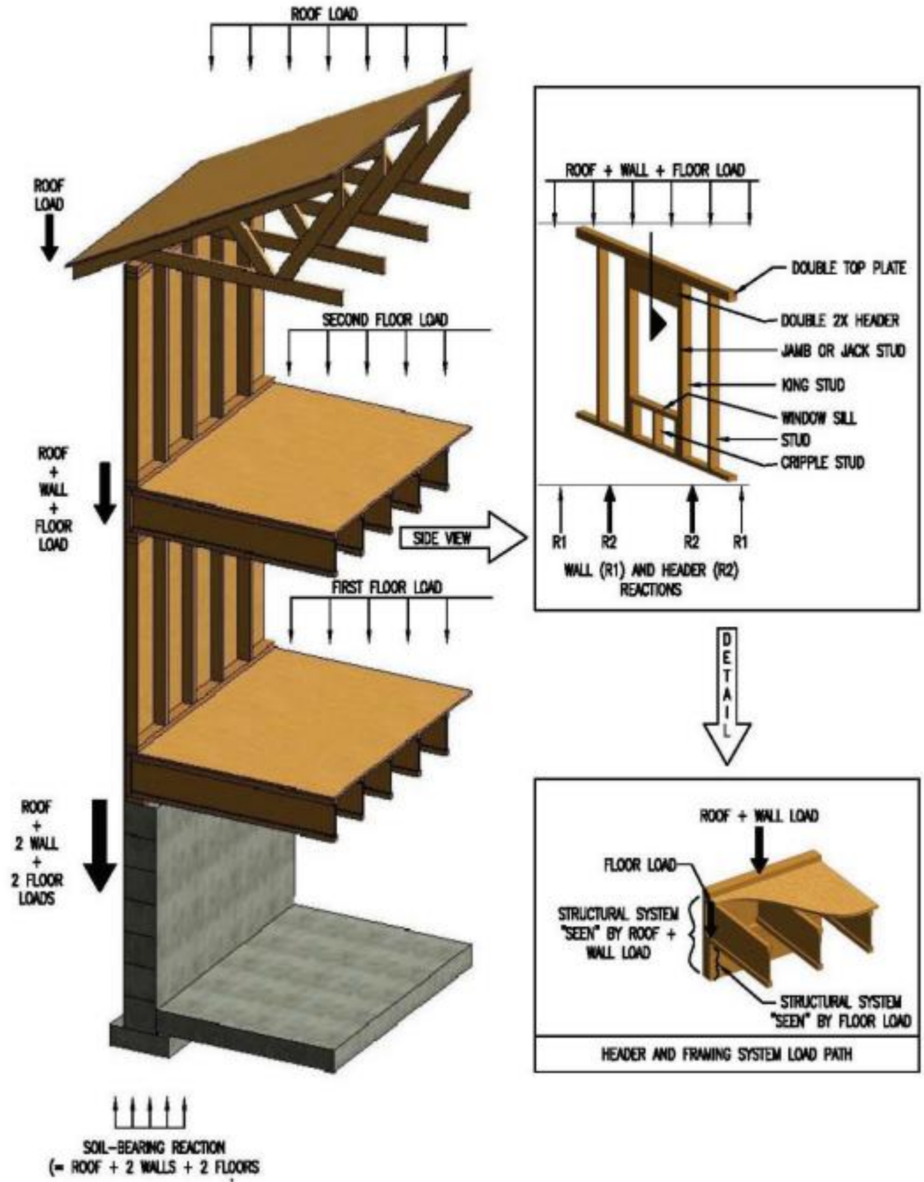

Figure 38. *Vertical Load Path for Gravity Loads [27]*

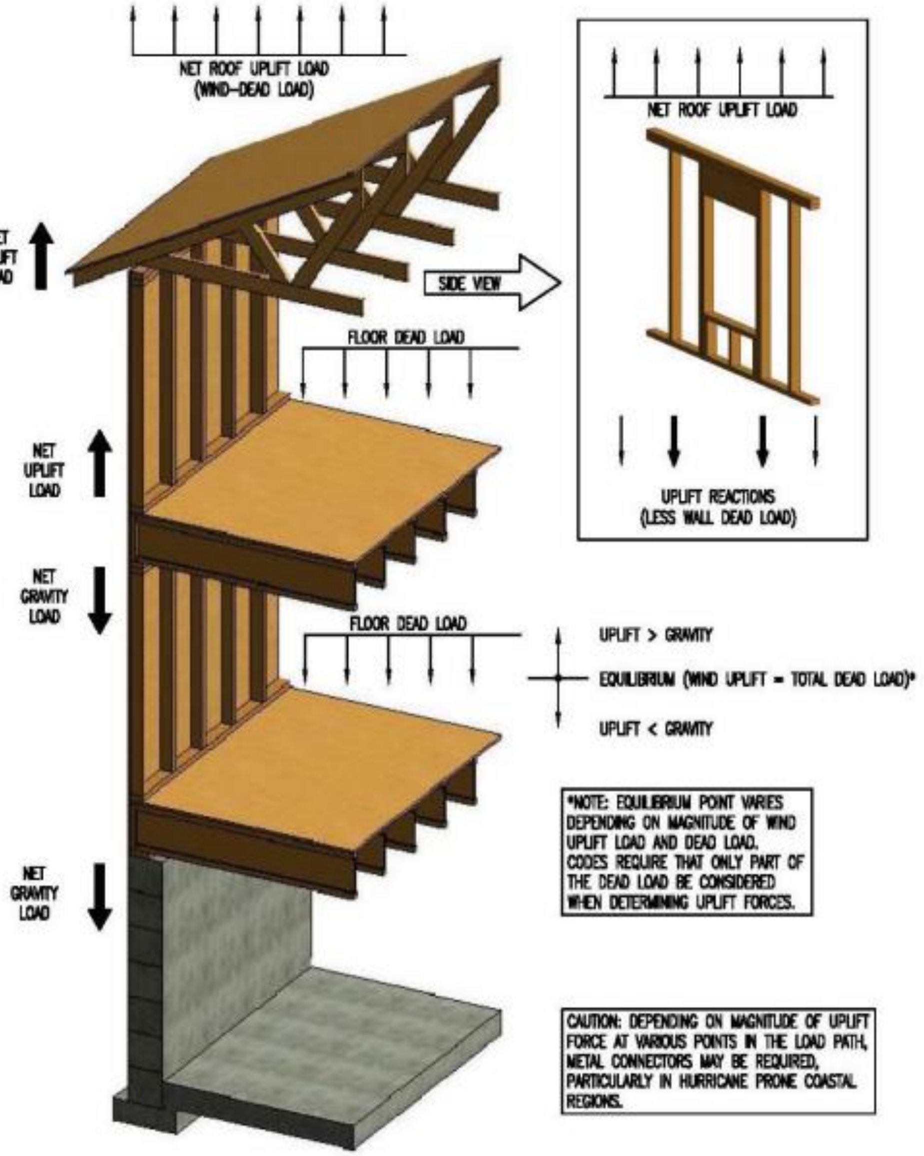

Figure 39. *Vertical Load Path for Wind Uplift [27]*

Dead Loads : Dead loads consist of permanent loads of building material from roof, floor, wall, and foundation systems, including cladding, finishes and fixed equipment. [27]. The values for dead loads shown below at table 6.

Table 6. *Dead Loads for Common Residential Construction [27]*

Conventional clay/tile roofing	27 pfs (1.293 kN/m^2)
Lightweight tile	21 pfs (1.005 kN/m^2)
Metal roofing	14 pfs (0.670 kN/m^2)
Wood shakes	15 pfs (0.718 kN/m^2)
Tar and gravel	18 pfs (0.862 kN/m^2)

After examining the dead loads, a structural analysis will be made on the metal roofing in our design. While performing this analysis, the easyPV tool, which is used for structure analysis in PV systems, will be used. As seen in figure 40, the weight of the solar array is taken 305.6 kg, because in our design PV modules' weight is 19.10 kg (given in figure 16) and our number of modules is 16. (16*19.10=305.6 kg). After that the area of solar panel design will be entered into the tool, then the weight of the mounting structure is assumed as 550 kg. Permitted dead load for metal roofing is taken 0.670 kN/m^2 from table 6.

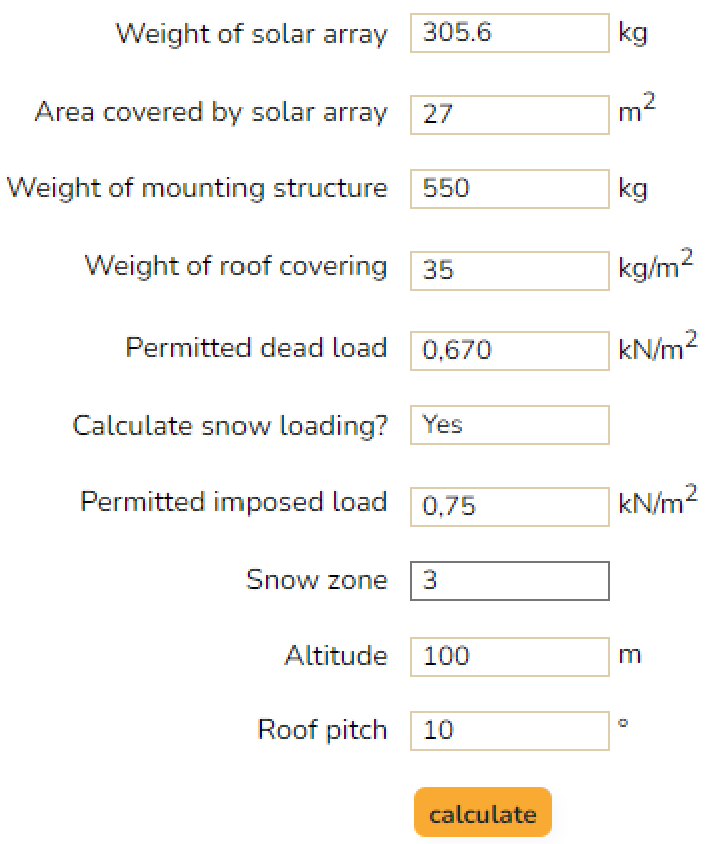

Figure 40. *Weight Loading Calculation on easyPV Tool*

The necessary calculations are made with the values entered into the easyPV tool and the structural analysis of the design is created as seen in figure 41.

Structural calculations

Weight loading calculations

Roof 1

Weight of solar panels and mounting	855.6 kg
Area of solar array	27 m^2
Loading imposed by solar array	0.31 kN/m^2
Dead load from roof covering	0.34 kN/m^2
Total dead load of solar array, mounting and roof covering	**0.65 kN/m^2**
Permitted dead load	**0.67 kN/m^2**

The solar array, mounting system, and roof covering are expected to impose a total dead load on the roof of **0.65kN/m^2**. This is less than the permitted dead load for the roof of **0.67kN/m^2**.

Snow Loading

Snow zone	3
Altitude	100
Roof pitch	10
Total imposed load of solar array, mounting and snow	**0.71 kN/m^2**
Permitted imposed load	**0.75 kN/m^2**

The maximum combined imposed loading from the solar array, mounting and snow is expected to be **0.71 kN/m^2**. This is less than the design imposed load for a truss roof of **0.75 kN/m^2**.

Figure 41. *Structural Calculations of the Design*

As seen from the results, the total weight of solar panels and mounting is 855.6 kg which is equal to 8390.57 N. (1 kg is taken 9.80665 N). When we divide 8390.57 by 27, we get 310.75 N/m^2 which is 0.31 kN/m^2. It simply explains how this easyPV tool creates equations and calculates results.

10. CONCLUSION

A review of the major solar photovoltaic technologies consisting of PV power generation is discussed. It is underlined that there are enormous renewable energy sources available and solar energy is one of them for electricity generation. This requires PV cells to be placed on building facades or roofs. This will lead to a reduction in power outages and greenhouse gas emissions. Increasing environmental concerns and the need to meet emissions reduction targets should help further establish the technology as a marketable and economically viable product. Also, government policies and research need to be implanted in the development of new solar technology. This article will be useful for solar PV system manufacturers, academics, researchers, producer members, and decision-makers.

REFERENCES

[1] Güneş Enerjisi ile Elektrik Üretimi. (2018) https://www.enerjiatlasi.com/haber/gunes-enerjisi-ile-elektrik-uretimi-3-kat-artti

[2] Sezal, L. (2017). Evaluation of the Solar Energy Investments in Turkey from Behavioral Finance. Journal of International Social Research. 10(51), 1117-1125.

[3] Melikoglu, M. (2016). The role of renewables and nuclear energy in Turkey′ s Vision 2023 energy targets: Economic and technical scrutiny. Renewable and Sustainable Energy Reviews, 62, 1-12

[4] Türkiye Ulusal Yenilenebilir Enerji Eylem Planı (2019). https://kusip.gov.tr/kusip/yonetici/tematikAlanEkGoster.htm?id=75

[5] Güneş enerji Potansiyeli Atlası (GEPA) (2019). http://www.eie.gov.tr/MyCalculator/Default.aspx

[6] Hantula R., (2010). How Do Solar Panels Works, Chelsea Club House, New York.

[7] Linden D. Ve Reddy T.B. (1995). Handbook of Batteries, Third Edition, McGraw-Hill, New York

[8] Podder Sh, Raman Khan Md.Z (2016). Comparison of Lead acid and Li-ion Battery in Solar Home System of Bangladesh", 5th International Conference on Informatics, Electronics and Vision

[9] Krismadinata, Abd.Rahim N, Wooi Ping H, Selvaraj J, (2013). Photovoltaic module modeling using simulink/matlab

[10] Saha Ch, Agbu N, Jinks R ve Huda M.N, (2018). Review Article of the Solar PV parameters Estimation Usibg Evolutionary Algorithms. MOJ Solar Photoen Sys. 2018

[11] Khezzar R, Zereg M and Khezzar A (2014). Modeling improvement of the four-parameter model for photovoltaic modules". Solar Energy

[12] https://www.mgm.gov.tr/FILES/resmi-istatistikler/parametreAnalizi/Turkiye-Gunluk-Guneslenme-Suresi.pdf

[13] https://www.mgm.gov.tr/FILES/resmi-istatistikler/parametreAnalizi/Turkiye-Yillik-G%C3%BCnes-Radyasyonu.pdf

[14] https://solargis.com/maps-and-gis-data/download/turkey

[15] https://pssdistributors.com.au/what-is-the-difference-between-square-wave-and-pure-sine-wave-inverters/

[16] https://www.aurorasolar.com/blog/solar-panel-types-guide/

[17] https://unboundsolar.com/

[18] https://www.ngdc.noaa.gov/

[19] Oral M. (2020). Türkiye'nin Güneş Enerjisi Potansiyeli ve PV Uygulamalarının Yerel Ölçekte Değerlendirilmesi: Karabük İli Örneği

[20] Küçükkaya E. (2016). Güneş Enerjisi Nedir, https://www.enerjiportali.com/gunes-enerjisi-nedir-4/ , 17 Ekim 2020.

[21] Hossaini M. (2021) Afganistan'da Konut Uygulamalari İçin Li-İon Pil Depolu Fotovoltaik Sistem Tasarimi Ve Optimizasyonu, Bolu Abant İzzet Baysal Üniversitesi Lisansüstü Eğitim Enstitüsü, Bolu, Türkiye.

[22] Su, Q., Zhang, G., Lai, J., Feng, S., Shi, W. (2010), Green Solar Electric Vehicle Changing the Future Lifestyle of Human

[23] Nna CD, Gbadegesin AO, Lawal KO. A Decentralized , Renewable-Energy-Powered Business Hub for Rural Areas : A Case Study of Ilakan Community , Nigeria 2013

[24] https://www.suncalc.org/#/40.1895,29.1221,7/2021.10.31/12:15/1/3

[25] Yıldırım E. , Aktacir M. (2020). Determination of Rooftop PV Electricity Generation Potential: The Case of Şanlıurfa.

[26] Dwyer S., Harper A., Lindau W., Bosiljevac T., Schindel K., Richards E. (2011), Structural Considerations for Solar Installers.

[27] Coulbourne, C, 2017 Residential Structural Design Guide A State-of-the-Art Engineering Resource for Light-Frame Homes, Apartments, and Townhouses (2nd edition)

[28] Hansen, C.: Estimating parameters for the PVsyst version 6 photovoltaic module performance model. SAND2015-8598. Sandia National Laboratories, Albuquerque (2015)